

**"Dunărea de Jos" University of Galați
Doctoral School of Fundamental Sciences
and Engineering**

**STUDIES ON THE PROCESS OF
OXIDATIVE DISSOLUTION
OF METAL SULFIDES**

Abstract

**PhD
Duinea Ionela-Mădălina**

**Scientific leader,
Prof. Dr. habil. Geta Cârâc**

**Series I 5: Materials Engineering, no. 16
GALAȚI
2020**

Contents		Pag
Contents		5
List of figures		8
List of tables		12
List of schemes		13
Symbols and abbreviations		14
Introduction		16
DOCUMENTARY PART		
1. Current state of environmental pollution due to mining activities and remedies		18
1.1. Environmental pollution due to mining		18
1.2. Impact of metal sulphide oxidation on the environment		21
1.2.1. Mining acid drainage (DAM)		21
1.2.2. Methods of remediation of acid drainage		22
1.3. Procedures for remedying for metal sulfide oxidative processes		24
1.3.1. Inhibitors - remedies methods		25
1.3.2. Organic inhibitors - effective solutions for inhibiting the oxidative process		25
1.3.3. Current state of use of organic inhibitors for metal sulfide oxidative processes		26
1.4. Processes for remedying acid mine drainage by obtaining new materials with applications in environmental protection		35
1.4.1. Modern approaches to remediation of heavy metal pollution from mining		35
1.4.2. Zinc sulfide nanoparticles as an efficient solution for heavy metal pollution		37
1.4.3. Remediation of heavy metal environmental pollution using zinc sulfide nanoparticles		40
1.5. Conclusions		43
1.6. Bibliography		44
EXPERIMENTAL		
Main objectives in the scientific studies		52
2. Characterization materials, methods and techniques		52
2.1. Materials used in the study of metal sulfide oxidation		53
2.1.1. Sphalerite (ZnS)		53
2.1.2. Troilite (FeS)		54
2.1.3. Chalcopyrite (CuFeS ₂)		55
2.1.4. Galena (PbS)		56
2.2. Organic inhibitors - synthesis and characterization		56
2.2.1. Phenacyl derivatives		57
2.2.2. Schiff bases grafted with TRIS units		59
2.2.3. Glycine		59
2.3. Quantum calculation methods applied for the study of metal sulfide oxidation		59
2.3.1. Energy characteristics and implications of phenacyl derivatives (DFs) in the oxidation process to ZnS		62
2.3.2. Energy characteristics and implications of glycine in the oxidation process to FeS		64
2.3.3. Energy characteristics and implications of the Schiff base grafted with TRIS units (ST1) in the oxidation process to FeS		65
2.3.4. Evaluation of the oxidation process of CuFeS ₂ using phenacyl derivatives (DFs) by quantum calculations		67
2.4. Preparation of metal sulfide samples		67
2.4.1. Obtaining samples from ZnS and CuFeS ₂ for study with phenacyl derivatives		68
2.4.2. Obtaining FeS samples for glycine study		70

2.4.3. Obtaining PbS samples for study with Schiff bases grafted with TRIS units (STs)	71
2.4.4. Construction of working electrodes for electrochemical investigations	73
2.5. Techniques for characterizing the oxidative processes in metal sulfides and for their inhibition study	73
2.5.1. Electrochemical investigation methods	73
2.5.2. Non - electrochemical methods	76
2.6. Conclusions	78
2.7. Bibliography	79

RESULTS AND DISCUSSIONS

3. Characterization of the oxidation process for ZnS and inhibition of the process using phenacyl derivatives (DFs)	82
3.1. Structural characterization of ZnS-DF1, ZnS-DF2 and ZnS-DF3 samples	82
3.1.1. Characterization by Fourier Transform Infrared Spectroscopy (FTIR)	82
3.1.2. Characterization by Raman Spectroscopy	83
3.1.3. Characterization by Scanning Electron Microscopy (SEM)	84
3.1.4. Elementary characterization by Energy dispersive X-ray spectroscopy (EDX)	84
3.2. Inhibition of the ZnS oxidation process using phenacyl derivatives	85
3.2.1. Electrochemical evaluation by Potentiodynamic Polarization	85
3.2.2. Evolution of sulfate ion concentration [SO ₄ ²⁻]	87
3.3. Conclusions	88
3.4. Bibliography	89
4. Characterization of the oxidation process for FeS and inhibition of the process using glycine and a Schiff base grafted with TRIS units	91
4.1. Characterization of oxidative processes and FeS inhibition in the presence of glycine	91
4.1.1. Characterization of samples by Fourier transform infrared spectroscopy (FTIR)	91
4.1.2. Inhibition of the FeS oxidation process using glycine	92
4.1.3. Evaluation of the capacity of Fe ²⁺ and Fe ³⁺ ions in the solution at the interaction with glycine, by UV-vis spectroscopy analysis	92
4.1.4. Characterization of the oxidative process by electrochemical measurements	93
4.1.5. Structural Characterization by FeS Surface Optical Microscopy, before and after Electrochemical Experiments	98
4.1.6. Mechanism of FeS oxidation in the presence of glycine	100
4.2. Characterization of oxidative processes for iron monosulphide in the presence of a new Schiff base grafted with TRIS units	101
4.2.1. Analysis of the implications of the Schiff base grafted with TRIS units for the oxidation process of FeS	101
4.2.2. Evaluation of ST1 inhibition capacity by analysis of metal iron oxidation	101
4.2.3. Inhibition of the FeS oxidation process by electrochemical measurements	104
4.2.4. Structural Characterization by Optical Microscopy of the FeS Electrode, before and after Electrochemical Experiments	106
4.3. Conclusions	106
4.4. Bibliography	107
5. Characterization of the oxidation process for PbS and inhibition of the process by using schiff bases grafted with TRIS units	108
5.1. Structural characterization of PbS-ST1, PbS-ST2, PbS-ST3 and PbS samples	111
5.1.1. Characterization by Raman Spectroscopy	111
5.1.2. Characterization by Scanning Electron Microscopy (SEM)	112
5.1.3. Elementary characterization by Energy dispersive X-ray spectroscopy (EDX)	113
5.2. Inhibition of the oxidation process by electrochemical measurements	114

5.3. Conclusions	116
5.4. Bibliography	117
6. Characterization of the oxidation process for CuFeS ₂ and inhibition of the process by the use of phenacyl derivatives and schiff bases grafted with TRIS units	120
6.1. Characterization of oxidative processes for CuFeS ₂ using three phenacyl derivatives (DFs)	120
6.1.1. Structural characterization of CuFeS ₂ samples to inhibit the oxidation process using DFs	120
6.1.1.1. Characterization by Fourier Transform Infrared Spectroscopy (FTIR)	121
6.1.1.2. Characterization by Raman Spectroscopy	122
6.1.1.3. Characterization by Scanning Electron Microscopy (SEM)	123
6.1.1.4. Characterization by Energy dispersive X-ray spectroscopy (EDX)	124
6.1.2. Inhibition of the oxidation process using DFs	124
6.1.2.1. Potentiodynamic Polarization (PP)	125
6.1.2.2. Electrochemical Impedance Spectroscopy (EIS)	126
6.1.2.3. Evaluation of the concentration of sulfate ion [SO ₄ ²⁻] and total iron [Fe _{tot}]	128
6.2. Characterization of oxidative processes for CuFeS ₂ using three Schiff bases grafted with TRIS units	130
6.2.1. Structural characterization of samples by Raman Spectroscopy	131
6.2.2. Characterization by Scanning Electron Microscopy (SEM)	132
6.2.3. Compositional characterization by Energy dispersive X-ray spectroscopy (EDX)	132
6.2.4. Inhibition of the oxidation process by electrochemical measurements	133
6.3. Conclusions	134
6.4. Bibliography	136
7. Synthesis and characterization of ZnS nanoparticles using capture agents	139
7.1. Background	139
7.2. Synthesis of ZnS NPs	139
7.2.1. Materials used	139
7.2.2. Synthesis reaction in obtaining ZnS NPs	140
7.3. Structural and spectrochemical characterization of ZnS nanoparticles using TRIS and DF as capture agents	141
7.4. Structural characterization by X-ray diffraction (XRD)	142
7.5. Structural Characterization by Scanning Electron Microscopy (SEM)	142
7.6. Elemental analysis by Energy dispersive X-ray spectroscopy (EDX)	144
7.7. Structural Characterization by Fourier Transform Infrared Spectroscopy (FTIR)	146
7.8. Spectral properties specific to ZnS nanoparticles	146
7.9. Synthesis mechanism	148
7.10. Conclusions	149
7.11. References	150
8. Conclusion	152
8.1. Final conclusions	152
8.2. Personal contributions	157
8.3. Perspectives in future research	158
9. Dissemination of research results	159
9.1. Publications in ISI indexed journals	159
9.2. Publications in journals indexed in international databases	159
9.3. Awarding research results by UEFISCDI	159
9.4. Participation in national / international conferences	160
9.5. Activity in scientific research	162

INTRODUCTION

The environment and its protection is a major and always current issue, which concerns researchers around the world, through the impact that affects nature and human activities, the health of the population.

Environmental pollution by carrying out mining activities and the release of high concentrations of heavy metals is initiated by the process of oxidation of metal sulfides (MeS). One way to reduce the polluting impact on the environment is to find effective solutions to inhibit this process and nowadays, this issue should be given special attention.

In the doctoral thesis, studies are focused on finding new solutions to inhibit the oxidative process developed by natural mineral sulfides.

The main objectives of the doctoral thesis were established with reference to the study of the process of inhibiting the oxidation of some metal sulfides, by using new synthesized organic compounds, as well as obtaining and characterizing new materials based on metal sulfide.

The personal motivation that determined me to choose this topic was the desire to contribute to current studies on environmental protection.

The analyzed metal sulfides are those that contribute to the initiation of environmental pollution in areas with mining impact, these being: ZnS, FeS, PbS and CuFeS₂.

The organic compounds used as organic inhibitors were: phenacyl DFs derivatives and Schiff bases grafted with TRIS STs, new compounds, synthesized at the A.I.Cuza University of Iași.

Chapter 1, Documentary Study, summarized the theoretical aspects and the topicality of studies on the research of oxidation mechanisms of materials such as metal sulfides (MeS), as well as the importance of developing methods to inhibit this process.

The experimental part of the scientific approach is presented in Chapter 2, **Materials, methods and characterization techniques**, which presents the preparation of working materials, synthesis of new compounds, quantum calculation methods and modern techniques for structural characterization of samples and electrochemical oxidation process.

Chapter 3, **Characterization of the oxidation process for ZnS and inhibition of the process using phenacyl derivatives**, presents the experimental results on the structural characterization (XRD, SEM, FTIR, Raman Spectroscopy) of natural zinc sulfides samples in acidic environment (pH = 2.5), at 25°C, before and after contact with three organic compounds of the phenacyl derivatives class. The analytical study on the oxidation reaction of ZnS and the impact of phenacyl derivatives (DFs) was performed by electrochemical methods (PP) and by determining the ion concentration [SO₄²⁻], as a result of the oxidation reaction.

Chapter 4, **Characterization of the oxidation process for FeS and inhibition of the process using glycine and a Schiff base grafted with TRIS units**, presents experimental studies on the structural characterization (XRD, FTIR) of troilite samples (FeS) before and after contact with the two organic compounds: in acidic environment (pH = 2.5), at 25°C. The samples obtained were characterized using modern analysis techniques. The impact of organic compounds on the oxidation process of FeS was investigated by electrochemical techniques (PP, EIS, CV).

Chapter 5, **Characterization of the oxidation process for PbS and inhibition of the process using Schiff bases grafted with TRIS units**, presents experiments aimed at the oxidation process of galena, PbS, in the presence of three new Schiff bases grafted with TRIS units (ST1, ST2 and ST3). The oxidation process was analyzed by electrochemical techniques (PP, CV), in acidic solutions (pH = 2.5) of STs (1 mM) and at a temperature of 25°C.

Chapter 6, **Characterization of the oxidation process for CuFeS₂ and inhibition of the process using phenacyl derivatives and Schiff bases grafted with TRIS units**, presents

the experimental results on structural characterization (XRD, SEM, FTIR, Raman Spectroscopy) and evaluation of the process of inhibition of CuFeS_2 oxidation reaction of natural chalcopyrite, before and after contact with phenacyl derivatives and Schiff bases, in acidic solutions ($\text{pH} = 2.5$), at a temperature of 25°C . The oxidation process was evaluated by electrochemical tests (PP, CV).

In Chapter 7, **Synthesis and characterization of ZnS nanoparticles using new capture agents (TRIS and DF)**, are presented the synthesis by co-precipitation of zinc sulfide nanoparticles is obtained and their characterization by modern analysis techniques, following the use of new compounds organics, capture agents, improving their spectral properties, for various applications.

Chapter 8, **Final Conclusions**, briefly presents the main conclusions of the scientific results obtained, and Chapter 9 presents the **Dissemination of research results**.

The doctoral thesis entitled "Studies on the process of oxidative dissolution of metal sulfides" extends to 162 pages and is structured in two parts: the first part is about 30% of the entire volume of the paper, is the documentary study, and the the second part represents the experimental part with original results, personal contributions in the approached field.

The bibliographic references are presented on each chapter, over 290 references / publications studied, of which 16 publications in which I am co-author or main author.

The paper includes 98 figures, 26 tables and 7 diagrams.

I believe that the results obtained and presented in the thesis can be an initiating benchmark, which should encourage further studies on metal sulfides, in finding viable and sustainable solutions for environmental protection.

1. DOCUMENTARY

Metallic minerals were an initiating stage in the development of mankind, their genesis being difficult to understand, they are governed by specific laws. Minerals such as those containing metals in their composition (ZnS , FeS , CuFeS_2 , PbS), have been and are with multiple applications. Metal sulfides (MeS) are abundant in nature, are a major source of metals and of great economic interest [1-5].

Iron monosulfides, chalcopyrite, galena and sphalerite are common in nature, and their presence along with other minerals can lead to both inefficiency in separation and serious environmental problems, such as acidic (or mining) rock drainage, phenomenon characterized mainly by the presence of large quantities of heavy metals (Cd, Cu, Hg, As, etc.) in the water resulting from mine leaks. MeS are basic minerals for the extraction of precious metals (gold, platinum), and the mineral waste obtained from the corresponding processes is very rich in heavy metals (Cu, Pb, Al, Zn, Hg, Cd), which leads to environmental pollution [6].

Waste reactivity has profound implications for the environment. One of the most important chemical reactions developed by mineral sulfides is the oxidative dissolution reaction, which is of great importance in various industrial processes (acid mining drainage, remediation of areas where mineral waste is disposed of, metal extraction) or natural (natural sulfur cycles and iron).

It is known that acid mine drainage (DAM) is a process caused by the oxidative dissolution of mineral sulfides in mine dumps, the surface of which has been exposed to air, water and microorganisms. This phenomenon can also be encountered as a result of natural processes or activities associated with mineral exploitation, when minerals are brought to the surface.

The formation of secondary reaction products on the surface of sulfur, with the potential to form inert layers, lead to inhibition of the diffusion of oxidants to the surface, thus slowing down the oxidation process of these types of minerals [1-8].

Chemical analyzes play a particularly important role in these processes, being necessary both to achieve an efficiency of mining extractions and to ensure that the impact of these phenomena on the environment is minimal.

Oxidation of mineral sulfides occurs during the grinding process, when the particle size is reduced for flotation and involves a complex interaction between the solutions and the mineral surfaces. During the oxidation of metal sulfides, sulfur atoms go through several oxidation states, thus forming various sulfur compounds [3-8].

In view of these data, it is important to minimize the pollution effects caused by mining operations, which result in the removal of large amounts of heavy metals and sulfuric acid in the environment. One of the most used remediation / stopping methods is the introduction into the MeS oxidation reaction system of inhibitors that prevent the oxidation of these minerals, and the most effective are organic compounds [4-13].

2. EXPERIMENTAL

Objectives

Have the importance of protecting the environment, from studies conducted and reported for the oxidation process of metal sulfides, we considered it important to make scientific contributions to finding new solutions to inhibit the oxidative process by expanding research into new organic compounds than reported in the literature.

Among the metallic sulfides, with impact on the environment, the most widespread materials were chosen, these being: FeS, ZnS, PbS and CuFeS₂.

Among the organic compounds, which can act as organic inhibitors, in the oxidative process of metal sulfides, three phenacyl derivatives (DFs) corresponding to the structures C₁₃H₁₄N₂OS (4-Phenyl-2-N-morpholinyl-thiazole-**DF1**), C₁₅H₁₆NO₂S₂Br₂ 1- (3,5-Dibromo-2-hydroxyphenyl) -1-oxoethane-2-yl-**DF2**) and C₁₂H₁₃O₃S₂Br (1- (5-bromo-2-hydroxy-3) N-diethylthiothiobarbate -methylphenyl) -1-oxoethane-2-yl-**DF3**) and three Schiff bases grafted with TRIS units (STs) corresponding to the structures: C₂₀H₃₂N₂O₇ (**ST1**), C₁₁H₂₁NO₄ (**ST2**) and C₄H₁₁NO₃ (**ST3**), but also an unsynthesized organic compound, **glycine** (C₂H₅NO₂).

The experimental part of the scientific approach is presented starting with this chapter, which presents the preparation of working materials, the synthesis of new compounds as inhibitors, quantum calculations for oxidation and inhibition process parameters, and modern techniques for characterizing samples and oxidative processes.

The stages of the scientific approach in achieving the proposed objectives focused on:

- I. Documentation on the impact of oxidative processes of MeS, for the environment and finding optimal solutions, with favorable impact (chapter 2).
- II. Study on the evaluation of the inhibitory effect due to phenacyl derivatives (DFs) in the process of inhibiting the oxidative process to ZnS (chapter 3).
- III. Study on the evaluation of the inhibitory effect of glycine and a new Schiff base grafted with TRIS units (ST1) for the oxidation process to FeS (chapter 4).
- IV. Study on the inhibitory effect due to Schiff bases grafted with TRIS units (STs) in the process of PbS inhibition (chapter 5).

- V. Evaluation of the inhibitory effect due to phenacyl derivatives (DFs) and Schiff bases grafted with TRIS units (STs) in the process of inhibition of oxidation CuFeS_2 (chapter 6).
- VI. Synthesis and characterization of ZnS nanoparticles using capture agents (chapter 7).

The interdisciplinary researches performed on metal sulfides, with and without reaction inhibitors, to meet the proposed objectives, were performed using modern infrastructures in research laboratories belonging to: Electrochemistry Laboratory, Faculty of Sciences and Environment, "Dunărea de Jos" University of Galați (www.ugal.ro), Research Laboratory of the Faculty of Sciences, University of Craiova (www.ucv.ro), Organic Chemistry Laboratories of the Faculty of Chemistry, „Alexandru Ioan Cuza” University of Iași (www.uaic.ro), The National Institute of Materials Physics in Bucharest (<https://infim.ro>) and the Research Center for Applied Sciences in Craiova (<http://www.incesa.ro/#/>).

2. Characterization materials, methods and techniques

2.1. Materials used in the study of metal sulfide oxidation

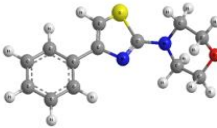
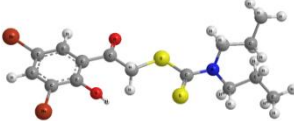
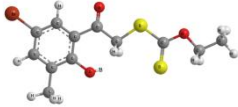
The materials needed for the study are the most important metal sulfides, which contain metals in their composition, such as: sphalerite, iron monosulfide, galena and chalcopyrite.



a-Sphalerite (ZnS), b-Troilite (FeS), c- Galena (PbS)
and d-Chalcopyrite (CuFeS_2)

In order to be used as organic inhibitors for the oxidative processes of metal sulfides, organic compounds of two distinctive classes were used, compounds of the phenacyl derivatives class (DF1 - $\text{C}_{13}\text{H}_{14}\text{N}_2\text{OS}$, DF2 - $\text{C}_{15}\text{H}_{16}\text{NO}_2\text{S}_2\text{Br}_2$ and DF3 - $\text{C}_{12}\text{H}_{13}\text{O}_3\text{S}_2\text{Br}$) and of a Schiff base. ST1 - $\text{C}_{20}\text{H}_{32}\text{N}_2\text{O}_7$, ST2 - $\text{C}_{11}\text{H}_{21}\text{NO}_4$ and ST3 - $\text{C}_4\text{H}_{11}\text{NO}_3$). The organic compounds were synthesized in the laboratories of organic chemistry, from the University of A.I. Cuza Iași.

Phenacil-derived compounds - IUPAC nomenclature,
chemical structure and molecular mass

DFs	Chemical structure
<p>DF1 C₁₃H₁₄N₂OS (4-phenyl-2-N-morpholinyl-thiazolyl) M=246 g/mol</p>	
<p>DF2 C₁₅H₁₆NO₂S₂Br₂ (1- (3,5-Dibromo-2-hydroxyphenyl) -1-oxoethan-2-yl N, N-diethyldithiocarbamate) M=437 g/mol</p>	
<p>DF3 C₁₂H₁₃O₃S₂Br (1- (5-Bromo-2-hydroxy-3-methylphenyl) -1-oxoethan-2-yl O-ethylxantogenate) M=317 g/mol</p>	

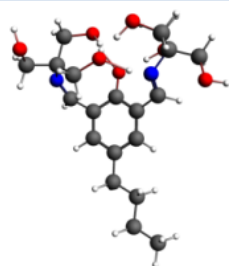
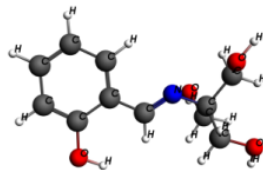
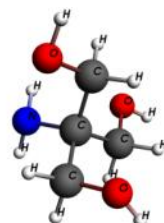
* carbon atoms (C) - gray; oxygen atoms (O) - red; nitrogen atoms (N) - blue, sulfur atoms (S) - yellow, bromine atoms (Br) (largest spheres) - red-brown; hydrogen atoms (H) (smallest spheres) -white.

These compounds have similar structures, by the presence of N and O heteroatoms on a chain of at least 2 carbon atoms. It also has an aromatic nucleus and an OH group attached to the aromatic nucleus.

Structural differentiations (two N atoms and one S atom, on the DF1 structure; two S atoms, one N; two Et-OH groups and two Br atoms on the DF2 structure and one Et-OH group, two S atoms as well as a Br atom on the DF3 structure) positions these organic compounds, according to quantum calculations, as effective inhibitors for the oxidation reaction to MeS, such as ZnS and CuFeS₂.

The Schiff bases show some structural differences such as: the aromatic nucleus (existing in the structure ST1 and ST2) and the different number of N and O atoms, which increases in the order: ST3 (1 atom of N and 3 of O) <ST2 (1 atom of N and 4 of O) <ST1 (2 atom of N and 7 of O). Said Schiff bases are used in the oxidation process of natural samples of PbS, CuFeS₂ and synthesized FeS samples (ST1).

Schiff bases grafted with TRIS units (STs),
chemical structure and molecular mass

STs	Chemical structure
ST1 $C_{20}H_{32}N_2O_7$ M = 412,4 g/mol	
ST2 $C_{11}H_{21}NO_4$ M = 233 g/mol	
ST3 $C_4H_{11}NO_3$ M = 121 g/mol	

* Atom color: carbon atoms (C) - gray; oxygen atoms (O) - red; nitrogen atoms (N) - blue, hydrogen atoms (H) (smallest spheres) - white.

Glycine ($C_2H_5NO_2$) was used in the study of synthesized FeS oxidation, offering the possibility to inhibit the oxidation reaction due to the O and N atoms in its structure. The glycine (99.9%) used was a product obtained from Merck. It is of interest for the study of MeS oxidation, having the smallest chain, consisting of 2 C atoms [1].

2.2. Quantum calculation methods applied for the study of metal sulfide oxidation

In the study of oxidative processes in MeS, quantum calculations were performed using the Amsterdam Functional Density (ADF) program version 2016.104, and the data obtained processed by the zeroth-order regular approximation (ZORA).

The geometry of the structures and the electronic properties of the organic compounds were analyzed with the correlation and exchange potential PW91, and the numerical base double - zeta (DZ) [2,3].

It aims to obtain quantum parameters such as: dipole moment (μ), energy of the molecular orbital occupied with the highest energy level (E_{HOMO}), energy of the unoccupied molecular orbital with the lowest energy level (E_{LUMO}) and energy band ($\Delta E = E_{LUMO} - E_{HOMO}$) that will help to elucidate the mechanism of adsorption of organic matter on the tested mineral surface. The increase of the dipole moment (μ) simultaneously with the decrease of the energy band (ΔE) will indicate a good inhibition of the oxidation process of MeS.

In the case of CuFeS_2 , in order to better outline the inhibition process, the molecular geometry will be optimized by the local density approximation (LDA), and the electronic configuration of the active center will be described by a double-zeta set of Slater-type orbitals and the model Charge Model 5 (CM5).

The results obtained will contribute remarkably to the initiation of the scientific approach for these studies. The tested organic molecules have inhibition potential due to the active centers found in their structure, and by supplementing with the parameters and atomic models analyzed with the Amsterdam Functional Density (ADF) program will outline a better analysis of the study of inhibition of metal sulfide oxidation (MeS).

First, quantum calculations were performed for organic compounds and then for structures involving their action.

Energy characteristics and implications of phenacyl derivatives (DFs) in the oxidation process to ZnS indicate the adsorption of DFs to Zn atoms, as being energetically favorable ($E_{\text{ad}} < 0$).

We studied six adsorption structures that appear to be stable structures, the most stable being indicated by the adsorption of the compound DF1 on the atom Zn (2), and the most unstable structure being rendered by the adsorption of the same compound DF1 on the atom denoted Zn (1).

The results obtained from the quantum calculations performed justify the experiments proposed in order to improve the oxidative properties of zinc sulfide, using phenacyl derivatives with inhibitory role of the oxidative process [4].

Energy characteristics and implications of glycine in the oxidation process to FeS are of great value for E_{HOMO} which indicates that glycine tends to donate electrons to the free molecular orbitals of the FeS surface. The low value of the energy band (ΔE) argues for a good inhibition efficiency, because the electron removal energy from the last occupied orbital is low. This finding and the low value of the dipole moment ($\mu = 0.714$ / Debye) suggest that the interaction between glycine and FeS surface is moderate, but the low value of the energy band suggests an inhibitory effect. Glycine is expected to act as an inhibitor to the FeS oxidation reaction, but the inhibitory efficiency is moderate [1].

Energy characteristics and implications of the Schiff base grafted with TRIS units (ST1) in the oxidation process to FeS indicate a high energy for E_{HOMO} which suggests a good ability to donate electrons. This energy is distributed around the nitrogen-containing fragments, while LUMO energy is distributed mainly around the aromatic nucleus. Low energy band (ΔE) values are associated with high inhibitory efficiency.

From the observations obtained, the ST1 molecule is expected to act as an inhibitor for the oxidation reaction of FeS, due to the low value of the energy band, but the relatively small extension of the two boundary molecular orbitals (HOMO and LUMO) must also be considered. and possible steric hindrances, which may block the adsorption of ST1 on the FeS surface [5].

Evaluation of the oxidation process of CuFeS_2 using phenacyl derivatives (DFs) by quantum calculations indicates the adsorption of the DF3 molecule through the Fe atom, and the most unstable is the adsorption through the Cu atom.

The calculation performed with GGA - PW91 indicates a stable adsorption structure on the surface of chalcopyrite is DF2, bound to the surface of CuFeS_2 by means of the Fe atom. The most unstable adsorption structure is observed for DF3 bound to the sample surface via the Cu atom.

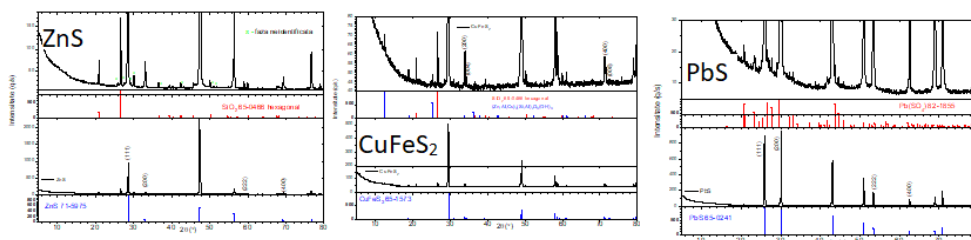
The calculated link lengths are: 2,320 Å for (DF) S-Cu (cluster); 2,363 Å for the Cu-S bond in the CuFeS_2 group; 2,300 Å (DF) S-Fe (cluster); and 2,201 Å for the Fe-S bond in the CuFeS_2 group.

These results encourage future studies for the mechanisms of action in identifying an inhibition process, regarding the oxidation reaction of CuFeS_2 using DFs.

2.3. Preparation of metal sulfide samples

2.3.1. Obtaining samples from MeS for study with organic compounds

It was used natural materials ZnS powder, CuFeS_2 , and PbS, respectively, FeS synthetic material, obtained from mineral purchased from Merck. X-ray diffraction analysis confirmed their structure [6-12].



X-ray diffractograms of the natural sample of ZnS (a), CuFeS_2 (b) and PbS (c)

ZnS și CuFeS_2 and DFs

The production steps consisted of finely grinding samples of MeS (ZnS or CuFeS_2) (8 g) in absolute ethyl alcohol (99.9% purity), dried for 48 hours in the desiccator, then by sieving the powder with a 125 μm . The necessary samples were obtained for the inhibitory investigation processes (5g).

For the treatment with DFs, in 4 Berzelius glasses were prepared 50 mL of alcoholic solution of organic compound DFs (DF1, DF2 and DF3) with a concentration of 1 mM, respectively, 99.9% ethyl alcohol. Weighed 4 samples of 1 g of MeS, obtained by the process described above, and in 3 samples the solution of organic compound DFs (1 mM) was added.

The mixture thus obtained was stirred magnetically at room temperature for 4 h. The product was decanted and dried in a desiccator for 48 h.

The result was the obtaining of some samples necessary to test the inhibition of the oxidation process at the ZnS surface, respectively at CuFeS_2 by chemical adsorption treatments with phenacil derivatives.

FeS and glycine

For the characterization of the unreacted / reacted FeS surface, working samples from FeS were prepared. FeS samples by contact with glycine were fine powders (dimensions 71 μm), after soaking in absolute ethyl alcohol (99.9%) and drying under vacuum for 1 h. Several samples were prepared in contact with air, 0,5 g FeS (fine powder) with a volume of 50 mL glycine solution (1 mM, pH 2,5 obtained with 1 M HCl), and 0,5 g FeS (fine powder) with a volume of 50 mL acid solution (pH 2.5 obtained with 1 M HCl). The mixtures thus obtained were stirred magnetically at room temperature for 4 h, and the product was decanted and dried in a desiccator for 48 h.

PbS and CuFeS₂ and STs

To characterize the metal sulfide (PbS and CuFeS₂) samples before and after contact with Schiff-based organic compounds (STs).

Approximately 7 g of natural metal sulfide (MeS) was ground in ethyl alcohol (99.9%), dried in a desiccator for 48 hours, and to obtain a fraction of 125 μm size it was sieved with a suitable sieve, using the Minor apparatus. M200 Endecotts. Duplicate tests were performed.

Weighed to the analytical balance, 1 g of finely ground MeS sample, and placed in 100 mL Berzelius beakers containing acidic solutions of STs (1 mM), pH 2.5 (obtained by dropwise addition of 1 N HCl).

The resulting mixture was magnetically stirred for 4 h at room temperature, the product was decanted and dried in a desiccator for 48 h.

The samples obtained marked with: MeS-ST1, MeS-ST2, MeS-ST3 and MeS, respectively, were characterized structurally by Scanning Electron Microscopy (SEM) and Raman Spectroscopy and compositionally by Energy dispersive X-ray spectroscopy (EDX).

2.4. Techniques for characterizing oxidative processes in metal sulfides and for their inhibition

Solid sample characterization techniques, such as MeS, involve two main types of analysis: structural analysis and analysis of oxidative properties on the surface of materials.

Structural analysis on the surface of mineral sulfides is performed using a variety of microscopic and spectroscopic techniques, while for the investigation of oxidative properties are used characterization techniques, electrochemical and non-electrochemical (dispersion techniques, microscopic techniques, spectroscopic techniques, etc.) [13 -16]. The analysis techniques used in the doctoral thesis, for the study of oxidative processes in MeS samples (ZnS, FeS, CuFeS₂ and PbS) in the presence of organic inhibitors (three phenacyl derivatives, three Schiff bases grafted with TRIS and glycine units).

Electrochemical investigation techniques, Electrochemical Impedance Spectroscopy (EIS), Potentiodynamic Polarization (PP), Cyclic Voltammetry (CV), very useful methods for the analysis of oxidation processes at MeS.

The electrochemical experiments were performed with the Zahner Zennim electrochemical station, with the Thales program, for data processing. An electrochemical cell with three electrodes was connected to the station:

- counterelectrode (CE) - a Pt foil (2 cm²)
- reference electrode (RE) - saturated calomel electrode (SCE); the results obtained being processed in relation to the Normal Hydrogen Electrode (SHE).
- working electrode (WE) - built according to the analysis method. Thus, coal paste electrodes and massive MeS electrodes, respectively, were used in the proposed study.

Working paste electrodes (CPE) [17], were built by depositing the powder obtained by specific treatments on a mixture of paraffin and graphite.

A 4 mm diameter Cu-insulated silicone wire as immersed in a mixture of 2 g graphite and 2.4 g paraffin heated to 75 °C. From the analyzed sample (ZnS, PbS and CuFeS₂) 0.02 g were introduced into a Teflon cavity with a diameter of 5 mm. The end of the Cu wire coated with the hot mixture of graphite and paraffin was immediately pressed onto the MeS particles placed in the Teflon cavity.

The result was a hemisphere with a diameter of about 4 mm made of a mixture of graphite and paraffin, covered by a very stable layer of sample, specific to MeS.

For the construction of solid electrodes, at the desired size, for FeS electrodes (Merck), a specific cutting device (Isomet Buehler-Germany) was used. The electrochemical behavior of

FeS in the presence of glycine was studied by obtaining working electrodes (EL) with an area of 1 cm^2 , to which a pre-experimental physical cleaning treatment was applied (the surface was sanded with SiC paper (600 and 1200 μm), and chemical (ultrasound in ethyl alcohol for 10 minutes) to remove fine particles that adhere to the electrode surface.

Working electrodes constructed of each metal sulfide were used for specific electrochemical investigations, Electrochemical Impedance Spectroscopy (EIS), Potentiodynamic Polarization (PP) and Cyclic Voltammetry (CV).

Non-electrochemical investigation techniques: modern structural and elemental analysis techniques for the sample surface, using X-ray diffraction (XRD), Scanning Electron Microscopy coupled with Energy dispersive X-ray spectroscopy (SEM / EDX), Fourier transform infrared spectroscopy FTIR), and Raman Spectrometry, useful for characterizing MeS with / without inhibitor.

RESULTS AND DISCUSSIONS

3. Characterization of the oxidation process for ZnS and inhibition of the process using phenacyl derivatives (DFs)

This chapter presents experimental results on the structural characterization by modern analysis techniques of natural zinc sulfide samples by treatment with new organic compounds, from the class of phenacyl derivatives.

The analytical study on the impact of phenacyl derivatives (DFs) on the oxidation reaction of ZnS with DFs, in acidic environment of pH 2.5 and 25°C , was performed by electrochemical investigations and determination of ion concentration $[\text{SO}_4^{2-}]$.

3.1. Structural Characterization by Fourier Transform Infrared Spectroscopy (FTIR) and Raman Spectroscopy

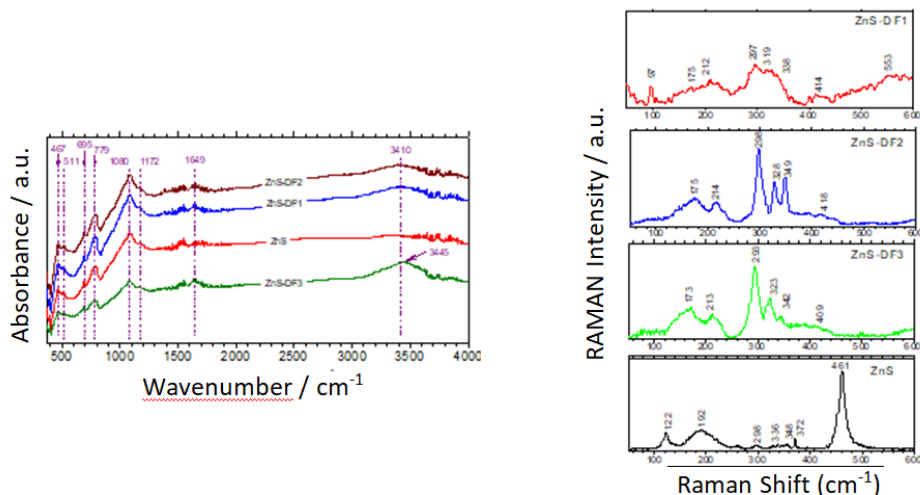
FTIR analysis indicates the presence of absorption bands at the wave number of 467 cm^{-1} , which can be attributed to the bonds of DFs compounds with sulfur, disulfides and polysulphides on the sample surface [18-22].

Compounds DF1 and DF2 (from samples ZnS-DF1 and ZnS-DF2) show stability with the ZnS surface through the S-N, S-O and S-S bonds, while the compound DF3 (ZnS-DF3 sample) has S-S and S-O bond, respectively. The peak recorded at 511 cm^{-1} and the present one at 3445 cm^{-1} are attributed to the oxygen-iron bonds (iron oxides) on the surface of the samples. At the position of 3445 cm^{-1} a visible increase is notable for the ZnS-DF3 sample, which has in its molecule 4 oxygen atoms that can react with the iron in the natural ZnS structure (4.1% proved by EDX analysis).

The position of the bands at 695, 1080 and 1172 cm^{-1} is attributed to the presence of sulfite, thiosulfate and sulfate. $\text{Fe}(\text{OH})_3$ formation and their presence on the ZnS surface is highlighted in the region from 779 cm^{-1} to 3400 cm^{-1} . The peak at 1649 cm^{-1} is attributed to the H-O-H bonds [23,24].

Raman spectroscopy shows adsorption bands corresponding to the ZnS sample found confirmed at 122, 192, 298, 336, 348, 372 and 461 cm^{-1} . Raman peaks at 336 and 348 cm^{-1} are specific bands for $\text{Fe}_x\text{Zn}_{1-x}\text{S}$ ($x = 0$). The first peak (336 cm^{-1}) is attributed to the FeS vibration band [25], while the second (348 cm^{-1}) is attributed to the ZnS vibration band [26]. It should be noted the increase of their relative intensity after contact with phenacyl derivatives (ZnS-DF1, ZnS-DF2 and ZnS-DF3) which can be associated with the formation of reaction products through Fe-O, S-O, Zn-O bonds. Polysulfides and elemental sulfur present on the ZnS surface

are characterized by an intense peak at 461 cm^{-1} [27], which disappears after interaction with organic solutions.



FTIR spectra and Raman spectra for the samples ZnS-DF1, ZnS-DF2, ZnS-DF3 and ZnS

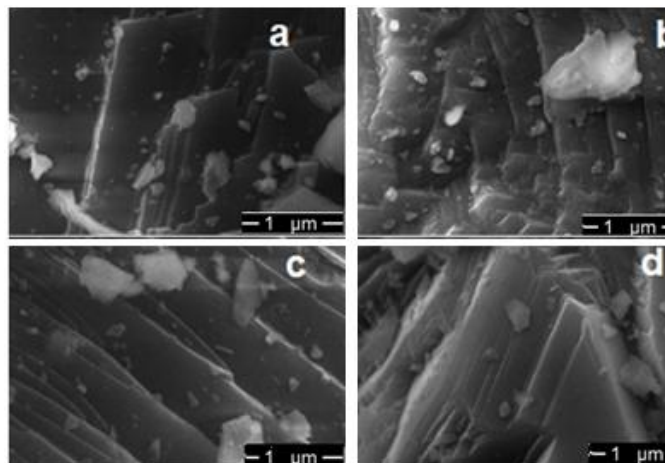
This modification confirms the binding of organic compounds to the ZnS surface, through sulfur species in the DFs structure through S-O, S-Fe, S-S type bonds.

The decrease of the Raman peak attributed to the vibration band, from 122 to 97 cm^{-1} , which is noticed only in the case of the ZnS sample treated with the DF1 solution, can be associated with the ZnS bonds with sulfur, through SS and SO bonds, respectively, forming reaction which may act as inhibitors for the oxidation reaction at the ZnS surface or may precipitate in solution.

Variations in the position of the recorded bands, in the Raman spectra, but also in the FTIR spectra, indicate that in the presence of phenacyl-derived organic compounds (DF1, DF2 and DF3) reaction products are formed which can form a protective oxidation barrier for the ZnS surface.

3.2. Structural Characterization by Scanning Electron Microscopy (SEM) and Energy dispersive X-ray spectroscopy (EDX)

SEM images indicate the presence of flat areas with different morphologies, but also the existence of dispersed particles, relatively uniform on the mineral surface. The appearance of the obtained layer may be due to the obtaining methodology (grinding, washing), but also to the treatment applied to the fine powder of ZnS (by contact with DFs).



SEM images obtained on samples of ZnS-DF1 (a), ZnS-DF2 (b), ZnS-DF3 (c) and ZnS (d)

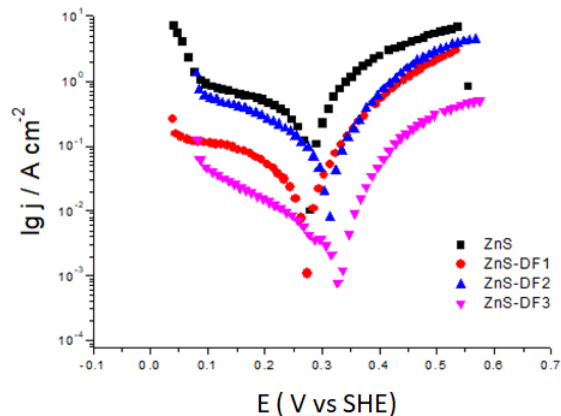
EDX analysis indicates elements such as sulfur, zinc, iron (approximately 4%), silicon of 0.3% and cadmium of 0.7%. In samples treated with DFs, the S content is lower (by $1.7 \pm 4.6\%$) compared to the untreated samples, the Fe content is slightly increased (by $0.9 \pm 1.7\%$) and the Zn content appears with few changes.

3.3. Inhibition of the oxidation process to ZnS

Samples were obtained from natural ZnS powder and phenacyl DFs-derived compounds in ethanolic medium at an acidic pH of 2.5 structurally characterized by modern analysis techniques and electrochemically studied. Quantum calculations were initially performed and the inhibitory process of new phenacyl derivatives for the ZnS mineral surface was studied.

The phenacyl derivative DF2 indicates a high inhibitory efficiency, but quantum calculations on the ZnS surface indicate a complex reaction mechanism, involving chemisorption processes, and the steric hindrance can weaken the bond between the organic molecule and the sample surface, which would eventually lead to low yield. to inhibit the oxidation process.

Potential Dynamic Polarization (PP) curves were obtained for a scan rate of 1 mV / s, in the potential range $E = \pm 0.25V$ with respect to the Calomel Electrode (SCE), but all potential values are presented in relation to the Electrode Normal Hydrogen (SHE). To test the reproducibility of the measurements, all experiments were performed twice, each time using new electrodes and acid solutions, freshly prepared. Potentiodynamic Polarization curves were recorded on CPE electrodes in acidic solutions, pH 2.5, at 25°C.



Polarization Potentiodynamic curves recorded in acidic solutions (pH 2.5) at 25°C

The differences that appear in the profile of the PP curves can be attributed to the unevenness of the electrode surface, which results from the complex preparation process, being samples of natural ZnS (grinding, sieving, etc.).

The current densities (j) recorded on CPE decrease in the order: ZnS > ZnS-DF2 > ZnS-DF1 > ZnS-DF3, these being correlated with the inhibitory effect of the three tested phenacyl-derived organic compounds, established from quantum calculations.

Thus, the ZnS-DF3 sample records the highest inhibition effect ($j_{ox} = 3.87 \text{ nA}\cdot\text{cm}^{-2}$) of ZnS oxidation, followed by the ZnS-DF1 samples ($j_{ox} = 38.4 \text{ nA}\cdot\text{cm}^{-2}$) and ZnS -DF2 ($j_{ox} = 81.6 \text{ nA}\cdot\text{cm}^{-2}$) which acts as inhibitors with moderate efficiencies.

The decrease in anodic current densities observed on the polarization curves obtained for the ZnS-DF2 electrode indicates that the phenacyl derivative DF2 is a predominantly cathodic inhibitor, while the phenacyl derivative DF1 and the phenacyl derivative DF3, respectively, are classified as mixed inhibitors (density anodic current and cathodic current density decrease in the presence of the two organic compounds) [28].

The electrochemical parameters were extracted from the polarization curves by Tafel analysis and it was observed that the oxidation current density (j_{ox}) decreases in the order: **ZnS > ZnS-DF2 > ZnS-DF1 > ZnS-DF3**.

The results obtained by calculating the polarization resistance (R_p) indicate an increase from $157 \text{ }\Omega\cdot\text{cm}^2$ to $800 \text{ }\Omega\cdot\text{cm}^2$, for the ZnS sample treated with compound DF1, to $577 \text{ }\Omega\cdot\text{cm}^2$ for the sample treated with compound DF2, and, respectively, at $8940 \text{ }\Omega\cdot\text{cm}^2$, for the sample treated with compound DF3. The inhibitory efficiency of j_{ox} ($\eta_{j_{ox}}$) was calculated from the electrochemical parameters, and the results obtained indicated an efficiency of over 98.7% for the treatment applied to the ZnS sample using compound DF3, 87% for compound DF1 and 71% for compound DF2. The polarization resistance (R_p) was calculated, the values obtained helping to obtain the inhibition efficiency (η_{R_p}). The results indicate inhibition efficiencies in the order: **ZnS > ZnS-DF2 > ZnS-DF1 > ZnS-DF3**.

A justification could be found in quantum calculations, where it was observed that although it has a good inhibitory effect, the compound DF2 has the most complex reaction mechanism, which leads, as electrochemical studies show, to lower efficiencies than inhibition (71.0 - 75.4%) compared to other treatments applied to zinc sulfide.

4. Characterization of the oxidation process for FeS and inhibition of the process using glycine and a Schiff base grafted with TRIS units

This chapter presents experimental studies on the characterization of some samples from troilite (FeS) in contact with two organic compounds: glycine and a new Schiff base grafted with TRIS units (ST1).

The obtained samples are structurally characterized by modern analysis techniques, and the impact of the organic compounds analyzed for the oxidation process of FeS was investigated by electrochemical techniques, in acidic environment of pH 2.5 and at 25°C.

4.1. Characterization of oxidative processes and their inhibition using glycine

Samples of FeS purchased from Merck were obtained by contact with glycine (1 mM) and without glycine, respectively, in acidic solutions, pH 2.5 at 25°C. The morphology of the obtained samples, denoted FeS (FeS without glycine) and FeS-Gli, respectively, was investigated by Fourier transform infrared spectroscopy (FTIR).

4.1.1. Characterization of samples by Fourier transform infrared spectroscopy (FTIR)

From the FTIR analysis it was observed the presence of peaks at the wave number of 423 cm⁻¹, 1102 cm⁻¹, 1403 cm⁻¹, 1637 cm⁻¹, 2851 cm⁻¹, 2921 cm⁻¹ and, respectively, 3434 cm⁻¹. The positions of the bands are characteristic for the formation of the resulting reaction products, either by the interaction of the FeS surface with the atmosphere, in the case of the untreated glycine sample, or by the contact with the organic compound, for the FeS-Gli samples [29 - 31].

The peak at the position of 423 cm⁻¹ indicates the presence of elemental sulfur on the surface of the samples. The peak at 1102 cm⁻¹ can be attributed to S-O bonds and sulfate ion formation. The absorption bands recorded at 2800 cm⁻¹ and 3000 cm⁻¹ are specific for the stretching of Fe (OH)₃ and α-FeO bonds [31,32]. The spectrum of the FeS-Gli sample shows a peak at 1023 cm⁻¹ and two additional peaks, of low intensity, at 807 cm⁻¹ and 1262 cm⁻¹, attributed to the Fe (III) bonds to sulphate.

Compounds such as CO₂ and H₂O adsorbed on the mineral surface, are signaled by the position of the peaks at 1403 cm⁻¹ and 1637 cm⁻¹ and 3434 cm⁻¹, respectively, highlighted on the spectra of both samples. In conclusion, both the untreated and the glycine-reacted FeS sample show characteristic peaks of iron monosulfide. The presence of peaks associated with the formation of reaction products are more intense on the sample treated with the organic compound, thus suggesting the formation of a protective layer, which can act as an inhibitor for the oxidation of the FeS surface.

Spectrum data suggest that glycine may have an inhibitory effect on the oxidation reaction of the FeS surface.

4.1.2. Inhibition of the FeS oxidation process using glycine

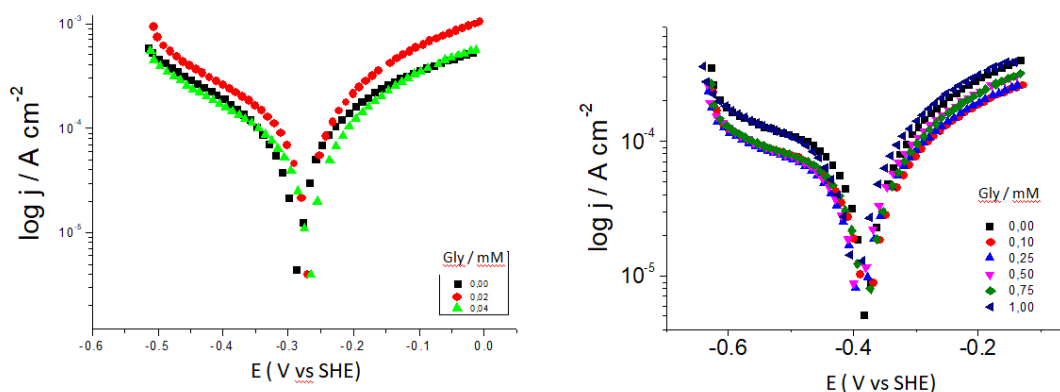
The adsorption mechanism is similar to that of metal corrosion and for this reason, we opted for the electrochemical investigation of this process, by the method of Potentiodynamic Polarization (PP).

Evaluation of the oxidation process of FeS in the presence of glycine was performed on two concentration ranges (0.02 and 0.04 mM and 0.10-1.00 mM), thus following the inhibition efficiency at low concentrations, and, respectively higher concentrations. The values were chosen so that the ratio of inhibition efficiency to inhibitory price is favorable for the oxidative process. The experiments were performed in an acidic environment (pH 2.5) at room

temperature. The pH is acidic because it has been shown that at $\text{pH} > 3$, Fe^{3+} (resulting from FeS oxidation) precipitates.

For studies of low glycine concentration range (0.02 and 0.04 mM) Potentiodynamic Polarization (PP) measurements were performed [4.9].

Tafel curves were recorded over a potential range, $E = \pm 0.25$ V in relation to the calomel electrode (SCE), the potential values being presented in relation to the Normal Hydrogen Electrode (SHE), and the scanning speed was of 10 mV / s.



Potentiodynamic Polarization curves obtained on the FeS electrode, in glycine solutions, at acidic pH (2,5) and 25°C

Before testing the effect of glycine for the oxidation of the FeS surface, experiments in acid solution without glycine were performed. After the addition of glycine, it was observed that the densities of the oxidation currents (j_{ox}) decreased from $60.2 \mu\text{A}\cdot\text{cm}^{-2}$ (0.00 mM) to $55.2 \mu\text{A}\cdot\text{cm}^{-2}$ (0.04 mM). This decrease is also evident in the profile of the polarization curves, confirming that the inhibition process is of mixed type. The oxidation potentials (E_{ox}) are approximately constant (a displacement of about - 0.01 V), which confirms that glycine acts as a mixed type inhibitor for the oxidation reaction of FeS [33].

At concentrations of 0.02 mM glycine, the densities of the oxidation currents (j_{ox}) indicate a higher evolution, from $60.2 \mu\text{A}\cdot\text{cm}^{-2}$ (0.00 mM) to $89.2 \mu\text{A}\cdot\text{cm}^{-2}$, causing thus an acceleration of the oxidation rate of FeS. Glycine, under acidic conditions (pH 2.5) and concentrations (0.02 mM or 0.04 mM), does not clearly indicate an inhibitory action and whether it can be considered an effective inhibitor for the FeS oxidation reaction. For these reasons, glycine was investigated over a longer concentration range (0.10-1.00 mM). The electrochemical study was performed by Potentiodynamic Polarization (PP) and Electrochemical Impedance Spectroscopy (EIS).

A decrease in the intensity of the oxidation current (j_{ox}) was found, which suggests that the oxidation mechanism of FeS is influenced by the presence of glycine in the reaction system.

The inhibition efficiency of glycine in the FeS oxidation reaction was calculated from the value of η_{jox} and the value of R_p .

Data obtained by polarizing the dynamic potential at the FeS electrode confirm that glycine, in the concentration range 0.10-1.00 mM, does not significantly alter the oxidation potential (E_{ox}), demonstrating mixed inhibitory effect [33].

In the concentration range up to 0.50 mM glycine, the oxidation current density (j_{ox}) decreases from $66.0 \mu\text{A}\cdot\text{cm}^{-2}$ (in the absence of glycine) to $38.7 \mu\text{A}\cdot\text{cm}^{-2}$ (0.50 mM glycine). Increasing the glycine concentration to 1.0 mM produces a slight increase in j_{ox} to $66.7 \mu\text{A}\cdot\text{cm}^{-2}$.

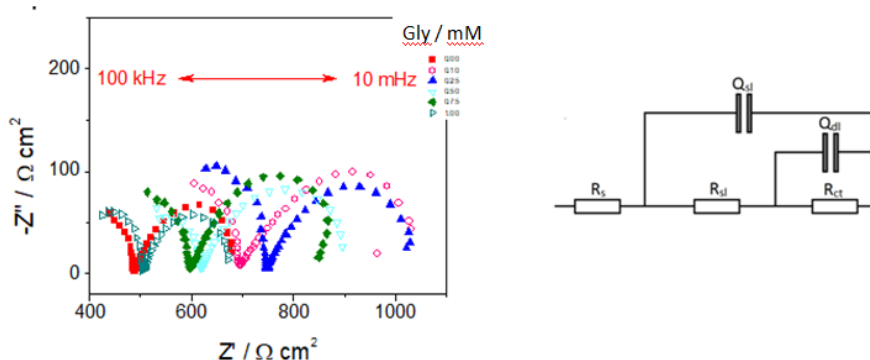
The calculated polarization resistance shows an increase from $3480 \text{ Ohm}\cdot\text{cm}^2$ to $7750 \text{ Ohm}\cdot\text{cm}^2$ for a glycine concentration of 0.50 mM.

Such a variation indicates that up to 0.50 mM, glycine is gradually adsorbed on the FeS surface producing a decrease in oxidation current density (j_{ox}) and implicitly, an increase in polarization resistance (R_p).

The inhibition efficiency calculated from j_{ox} ($\eta_{j_{ox}}$) for the FeS oxidation process, indicates up to a glycine concentration of 0.50 mM an inhibition efficiency of 41.4%, but a decrease for higher glycine concentrations (8% for $[\text{glycine}] = 1\text{mM}$).

The steps of the evolution of the inhibition efficiency are also supported by the inhibition efficiency calculated from R_p (η_{R_p}), indicating a percentage of 55.1% for the glycine concentration of 0.5 mM.

Electrochemical Impedance Spectroscopy (EIS) was performed over a frequency range of 100 kHz to 10 mHz with a signal amplitude of 10 mV. The data obtained were processed using Tales software.



Nyquist curves obtained on the FeS electrode, in glycine solutions, at pH 2,5, 25°C (a) and the equivalent electrical circuit used for the analysis of the impedance data (b)

The analysis of the Nyquist curves obtained in the absence and, respectively, the presence of glycine shows the appearance of an incomplete capacitive loop at high frequencies and, respectively, of a complete semicircular capacitive loop at low frequencies.

Incomplete capacitive loop is attributed to the formation of the surface layer composed of reaction products (elemental sulfur, polysulfides, ferric oxyhydroxides). The full capacitive semicircular loop can be attributed to the load transfer resistance (R_{ct}). The impedance parameters from the results obtained from the EIS experiments performed were modeled for an equivalent electrical circuit.

*Impedance parameters obtained for the electrode
FeS in glycine solutions, pH 2.5, at 25°C*

[Glycine] mM	R_{sl} Ohm·cm ²	R_{ct} Ohm·cm ²	R_p Ohm·cm ²	η_{Rp} %
0,00	487	214	701	-
0,10	713	419	1132	38,7
0,25	757	291	1048	33,1
0,50	624	298	922	23,9
0,75	601	293	894	21,5
1,00	505	183	688	-

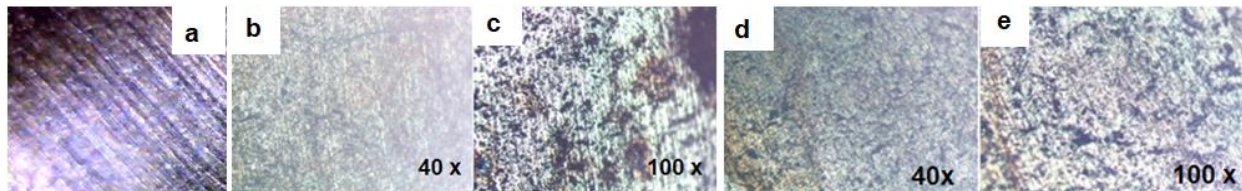
From the obtained data it is observed that R_r has an inverse tendency towards j_{ox} . At low glycine concentrations, R_r increases from 701 Ohm·cm² ([glycine] = 0.00 mM) to 1132 Ohm·cm² ([glycine] = 0.10 mM). R_p gradually decreases to 688 Ohm·cm² ([glycine] = 1.00 mM). Q_{dl} increases when glycine is added to the reaction system, while Q_{ct} decreases in the presence of the organic molecule.

The maximum standard deviation for the electrochemical impedance parameters is $\pm 1,9\%$.

4.1.3. Structural characterization by Optical Microscopy of the FeS surface, before and after electrochemical experiments

The characterization of the structural morphology by Optical Microscopy (MO) of the FeS surface before and after the electrochemical experiments was performed using the optical microscope with magnification of 40x, and 100x, respectively.

The FeS surface was analyzed before electrochemical experiments and after electrochemical experiments (PP) in acid solutions without glycine and [glycine] = 0.02 mM; [glycine] = 0.04 mM; [glycine] = 0 mM and [glycine] = 0.50 mM.



MO images at the surface of the FeS electrode, after pre-experimental treatment (a), after electrochemical experiments in solution without inhibitor, analyzed with the objective 40x (b) and 100x (c), after electrochemical experiments in solution of [glycine] = 0.02 mM : 40x (d) and 100x (e), at pH 2,5 and 25°C

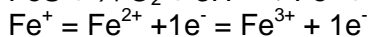
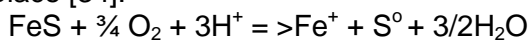
MO images show the decrease of traces after grinding and the appearance of small surfaces with chromatic differences, which are associated with the appearance of iron oxyhydroxides.

The FeS surface before and after the electrochemical experiments performed in glycine solutions ([glycine] = 0.02 and 0.04 mM) does not require further investigation. For a higher concentration, a more detailed analysis of the reaction products and the mechanism of action of glycine on FeS oxidation is required.

4.1.4. The mechanism of FeS oxidation in the presence of glycine

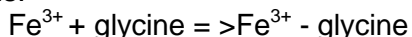
The ability of iron ions dissolved in solution (Fe^{2+} and Fe^{3+} ions found as a result of the FeS oxidation reaction) to interact with glycine was analyzed by UV-vis spectrophotometric analysis. A lack of interaction between Fe^{2+} and glycine ions was found, but a marked change at λ of 206 nm on the spectrum for Fe^{3+} and glycine indicates chemical interaction between the two components. By assimilating with the obtained data the quantum calculation shows the adsorption of glycine on the FeS surface, being influenced by the interaction between the HOMO orbitals of glycine with Fe^{3+} ions resulting from the oxidation of the FeS surface.

A possible oxidation mechanism of FeS in the presence of glycine includes several steps. When dissolved oxygen comes in contact with the FeS surface, the chemical reaction takes place [34]:

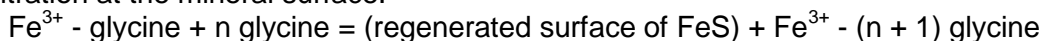


where S^0 is elemental sulfur, present as such or incorporated into polysulfide species. Divalent iron is subsequently oxidized to trivalent iron.

Glycine added to the reaction system is absorbed on the oxidized surface in Fe^{3+} species, reducing the value of j_{ox} (inhibition efficiency increases), results demonstrated by PP analysis.



The lowest j_{ox} value is obtained at the glycine concentration of 0.50 mM ($38.7 \mu\text{A}\cdot\text{cm}^{-2}$). The subsequent increase of the glycine concentration favors the dissolution of the Fe^{3+} ions present on the surface of the FeS samples and implicitly the decrease of the glycine concentration at the mineral surface.



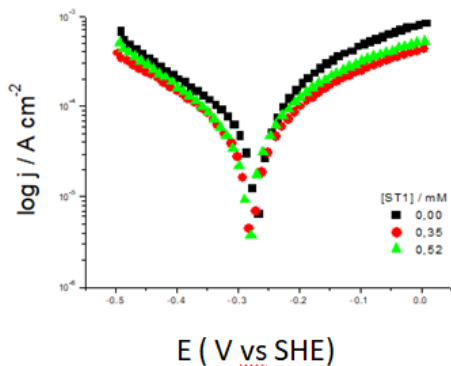
where: n is a small integer ($n = 2$ as suggested by UV-vis analysis).

Considering that glycine does not have a high capacity to adsorb directly on the FeS surface, the j_{ox} values will increase, the R_p values will decrease, and implicitly, the inhibition efficiency will be diminished.

4.2. Characterization of oxidative processes for iron monosulphides in the presence of a new Schiff base grafted with TRIS

4.2.1. Inhibition of the oxidation process of FeS by electrochemical measurements

Schiff base grafted with TRIS units offers the possibility of favorable electronic exchanges. The oxidation process of FeS was studied by electrochemical methods (PP and CV). The FeS (Merck) sample was analyzed by XRD which confirmed that it has the structure of a troilite.



[ST1] mM	E_{ox} V	j_{ox} $\mu A \cdot cm^{-2}$	b_a mV/dec	b_c mV/dec	R_p Ohm $\cdot cm^2$	η %	
						din j_{ox}	din R_p
0,00	-0,284	61,2	190	-216	7026	-	-
0,35	-0,286	43	220	-210	9302	29,7	24,4
0,52	-0,283	34,1	152	-163	16129	44,3	56,4

Polarization curves Potentiodynamics and electrochemical parameters obtained by Tafel analysis on the FeS electrode, in acidic solutions of ST1, pH 2.5, at 25°C

The electrochemical parameters were obtained by Tafel analysis, where E_{ox} is the oxidation potential, j_{ox} is the density of the oxidation current, b_a and b_c are the anodic and cathodic Tafel slopes, respectively.

The addition of ST1 to the reaction system, using the FeS electrode, decreases the j_{ox} from $61.2 \mu A \cdot cm^{-2}$ to $43 \mu A \cdot cm^{-2}$ (0.35 mM). Increasing the concentration of ST1 to 0.52 mM decreases the j_{ox} to $34.1 \mu A \cdot cm^{-2}$.

The obtained results demonstrate that up to a concentration of approximately 0.35 mM, the organic compound ST1 is adsorbed on the FeS surface, following that at a higher concentration it dissolves its surface, favoring the oxidation process.

E_{ox} does not change significantly when the ST1 concentration increases, suggesting a mixed type inhibitor role in the experienced organic compound [35].

The cyclic voltamograms obtained on the FeS electrode immersed in ST1 solutions show low anodic current densities when the solution of organic compound is added to the reaction system.

In contrast, at negative potential values, ST1 indicates the opposite effect on current densities (i_c). This behavior indicates a reduction in oxygen replaced by a reduction in polysulfide and elemental sulfur during FeS oxidation in the presence of the inhibitor.

The results also indicate oxidation from Fe(II) to Fe(III), and S(-II) to S(0) and S(+VI), respectively.

5. Characterization of the oxidation process for PbS and process inhibition using Schiff bases grafted with TRIS units

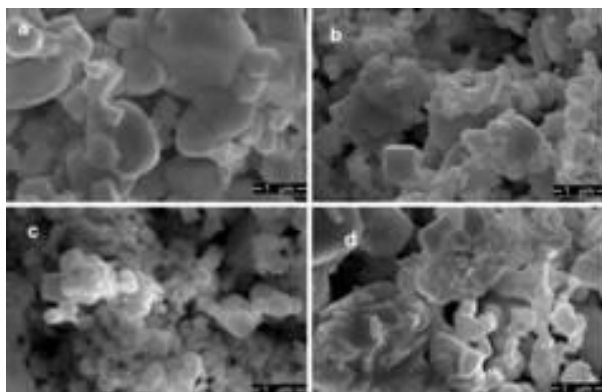
5.1. Structural characterization of samples

5.1.1. Characterization by Raman Spectroscopy

The Raman spectra in the analyzed samples show maximum intensities in the area $77 \text{ cm}^{-1} - 967 \text{ cm}^{-1}$. The PbS sample shows 3 vibration bands at 92 cm^{-1} , 138 cm^{-1} and 443 cm^{-1} , respectively, bands that are assigned to the Pb-S bonds [36]. After the interaction with some organic compounds, studies have shown the displacement of these bands, attributed to the transverse and longitudinal acoustic vibrational modes (LA + TA) of the cubic structure PbS [37-39].

5.1.2. Characterization by Scanning Electron Microscopy (SEM) and Energy dispersive X-ray spectroscopy

The SEM images taken from the PbS-ST1, PbS-ST2, PbS-ST3 and PbS samples show, on their surface, an agglomeration of particles, smaller or larger than 1 μm , due to the physical process on the mineral (processing by grinding), but and due to chemical treatment (treatment with STs).



SEM images obtained on samples of PbS-ST1 (a), PbS-ST2 (b), PbS-ST3 (c) and PbS (d)

Imaging of samples treated with organic compounds (STs) indicates a fragmentation of solids and dispersion over the entire surface, their uniformity indicating the formation of a layer of reaction products that can act as inhibitors of PbS oxidation.

The EDX analysis performed on the same samples of PbS-ST1, PbS-ST2, PbS-ST3 and PbS, respectively, together with the SEM analysis indicates the presence of the main elements of lead sulfide, lead and sulfur. It is observed that lead is in a higher percentage than sulfur, which can be explained by the fact that, after interaction with STs, sulfur species can be oxidized to sulfate and are precipitated in solution [40].

An increase in the percentage of Pb (1.06%) is observed, simultaneously with a decrease in the percentage of S (2.97%) for the sample treated with the organic compound ST2 (PbS-ST2), compared to the untreated sample (PbS). For samples treated with compounds ST1 (PbS-ST1) and ST3 (PbS-ST3), respectively, compared to the untreated sample (PbS), there is a decrease of $0.83 \pm 2.8\%$ for the percentage of Pb and, respectively, an increase of $0.23 \pm 1.63\%$ for the percentage of S, found at the mineral surface.

These values indicate both the formation of reaction products, such as lead oxide found on the reacted surface, and obtaining elemental sulfur that can precipitate in solution by decreasing the percentage of sulfur found on the mineral surface after contact with the organic compound [41].

5.2. Inhibition of the oxidation process by electrochemical measurements

Potentiodynamic Polarization (PP) and Cyclic Voltammetry (CV) studies were performed on PbS carbon paste electrode (CPE) in solutions of STs, pH 2.5 and 25°C.

The electrochemical study was performed in a classical cell with three electrodes, the equipment and methodology for obtaining working electrodes, carbon paste electrodes (CPE).

Potentiodynamic Polarization (PP) curves were obtained on the CPE-PbS electrode in acidic solutions of organic compound, ST1, ST2 and ST3, respectively, 1 mM, with pH 2.5.

It is observed that the density of the oxidation current (j_{ox}) decreases significantly on the cathodic area with the introduction of Schiff bases in the reaction system, thus demonstrating that the compound ST3 has the most obvious effect of cathodic inhibition, followed by the compound ST2 and the compound ST1. An increase in the density of the oxidation current on the anodic slope can be explained by the acceleration of PbS oxidation in the presence of Schiff bases, ST1 acting the least in this respect.

By Tafel analysis of the PP curves the electrochemical parameters were obtained.

From the recorded values, a decrease in the density of the oxidation current (j_{ox}) is observed in the PbS samples, from $226 \mu\text{A}\cdot\text{cm}^{-2}$ (in the absence of STs) to $87.4 \mu\text{A}\cdot\text{cm}^{-2}$, by using the compound ST1, of $51.1 \mu\text{A}\cdot\text{cm}^{-2}$ by using compound ST2 and of $17.0 \mu\text{A}\cdot\text{cm}^{-2}$, respectively, for compound ST3.

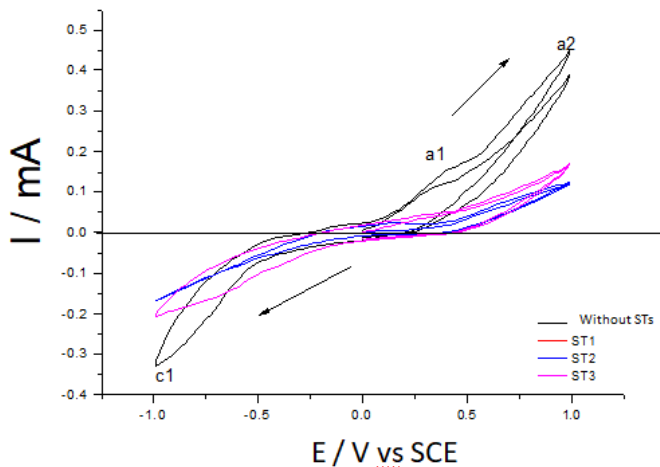
The inhibition efficiency ($\eta_{j_{ox}}$) from the j_{ox} values and from the polarization resistance (η_{Rp}) was calculated. The results obtained indicated that Schiff bases, with the structures of compounds ST1, ST2 and ST3, act as effective inhibitors for the oxidation reaction of PbS, in the order: **ST3 (> 92%) > ST2 (> 75%) > ST1 (> 60%)**.

The inhibition yield calculated from the j_{ox} ($\eta_{j_{ox}}$) values is 78%, and from the R_p (η_{Rp}) values over 75%, in the case of ST2, and for ST3, $\eta_{j_{ox}}$ is 93% and η_{Rp} is over 92%, the differences in the calculated yields in both ways being small, about 3-1%.

For the experiment performed in ST1 solutions $\eta_{j_{ox}}$ is over 60% and η_{Rp} is over 40%, the difference of about 20% in the values of calculation yields is explained by the high value recorded on the cathode slope for the CPE-PbS electrode in ST1 solutions.

Cyclic Voltammetry studies were performed on the CPE-PbS electrode in solutions of STs, pH 2.5 and 25 °C.

Cyclic voltammograms were recorded over an applied potential range of ± 1 V/SCE, with a scan rate of 100 mV/s.



Cyclic Voltammograms recorded on the electrode CPE-PbS in acidic solutions of ST1, ST2 and ST3 (pH 2.5), at 25°C

The recording of two peaks on the area of positive potential, in the voltammogram obtained in solution without Schiff base (a1 at $E = +0.38$ V / SCE and a2 at $E = +0.98$ V / SCE) indicates that the process of oxidation of the PbS surface, and the corroboration of their appearance with the decrease in the intensity of the oxidative current ($I_{a2} = +0.44$ mA) in the samples treated with STs compounds highlights the formation of reaction products obtained from the oxidative process [42,43].

In samples treated with STs compounds in solution, a bit corresponding to an oxidation current a1 no longer appears, indicating the formation of a protective layer on the mineral surface of PbS, by adsorption of Schiff bases grafted with TRIS units, having an inhibitory effect.

6. Characterization of the oxidation process for CuFeS_2 and inhibition of the process by the use of phenacyl derivatives and Schiff bases grafted with TRIS units

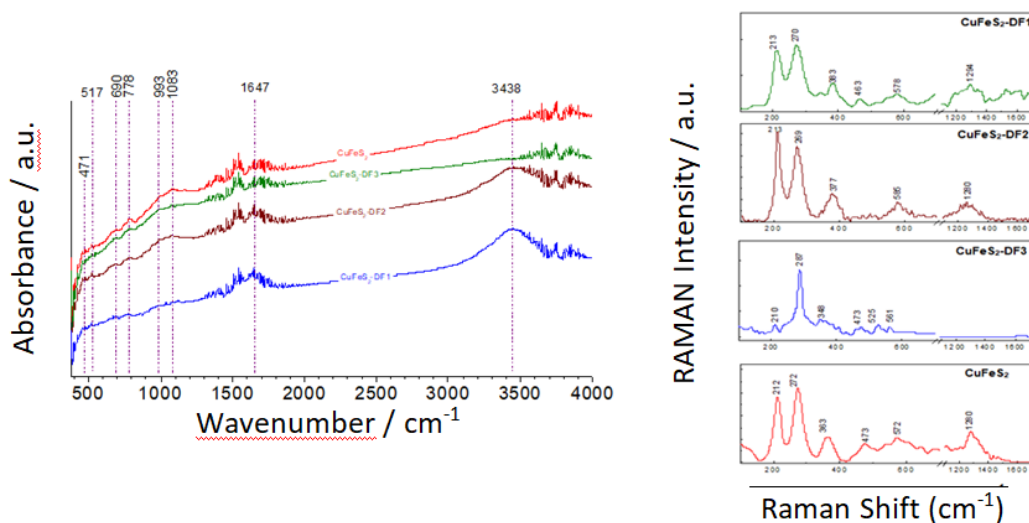
6.1. Characterization of oxidative processes for CuFeS_2 using three phenacyl derivatives (DFs)

Samples were obtained by contact with phenacyl derivatives, noted as follows: CuFeS_2 -DF1, CuFeS_2 -DF2 CuFeS_2 -DF3 and, respectively, without phenacyl derivative, CuFeS_2 .

The samples were structurally analyzed by Fourier Transform Infrared Spectroscopy (FTIR), Raman Spectroscopy and Scanning Electron Microscopy (SEM), and the compositional analysis by Energy dispersive X-ray spectroscopy (EDX).

6.1.1. Structural characterization of CuFeS_2 samples regarding the inhibition of the oxidation process using DFs

The FTIR analysis aimed to identify the phases present on the surface of the samples treated with phenacyl derivatives, noted: CuFeS_2 -DF1, CuFeS_2 -DF2 CuFeS_2 -DF3 and, respectively, without phenacyl derivative, CuFeS_2 . The recording of spectra in solid samples was performed over a spectral range from 375 to 4000 cm^{-1} , with a resolution of 2 cm^{-1} [20].



FTIR spectra and Raman spectra for CuFeS_2 -DF1, CuFeS_2 -DF2 CuFeS_2 -DF3 and CuFeS_2

In the spectral range 400-1100 cm^{-1} there are peaks that can be attributed to elemental sulfur species, for disulfides and polysulfides. At the peak of 471 cm^{-1} the S-O bond is identified, at the peak of 517 cm^{-1} the Fe-O bond is identified, at 690 cm^{-1} and 778 cm^{-1} the bonds in the

FeOOH and Fe (OH)₃ compounds are identified, respectively. Sulfite and sulphate bound to Fe (III) or Cu (II) are identified at the position of 993 cm⁻¹ and 1083 cm⁻¹, respectively.

The presence of peaks at 1647 cm⁻¹ is attributed to the deformation vibrations for H-O-H, and for Fe (OH)₃ at the position at 3438 cm⁻¹. It should be noted that the peak at this position is present in the spectra recorded in the samples treated with DF1 (CuFeS₂-DF1) and DF2 (CuFeS₂-DF2), respectively, but is missing in the spectrum obtained in the samples of CuFeS₂-DF3 and CuFeS₂, the peak being associated with the appearance of iron oxyhydroxides.

Raman spectra were also performed, which are evaluated as a complement to the FTIR technique. The analysis was also performed on samples of CuFeS₂-DF1, CuFeS₂-DF2, CuFeS₂-DF3 and CuFeS₂, respectively, and were not recorded over an interval of $\lambda=10-1700$ cm⁻¹.

The peaks identified by Raman spectroscopy are located in three distinct ranges, between 100-300 cm⁻¹, 400-600 cm⁻¹ and 1200-1400 cm⁻¹.

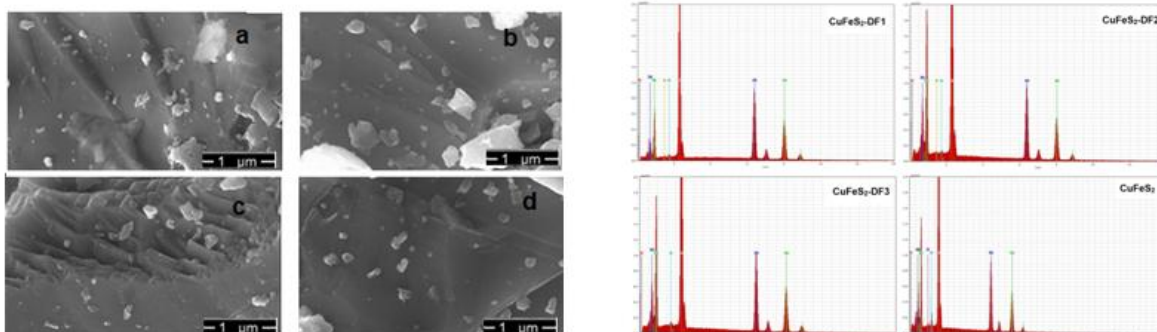
The signals responsible for the S-O and SO₄²⁻ bonds are found in the range of 500-700 cm⁻¹ and 100-300 cm⁻¹, respectively [44]. The spectral range 1200-1400 cm⁻¹ is attributed to the Fe-O, Cu-O bonds.

Thus, compound DF2 (CuFeS₂-DF2) and compound DF1 (CuFeS₂-DF1) show no spectral changes compared to the CuFeS₂ sample, but the peaks present in the spectra of these samples are associated with the formation of reaction products that can act as inhibitors for the oxidation process. of the studied metal sulfides. The changes in the sample treated with compound DF3 (CuFeS₂-DF3), is reflected in the decrease of the relative intensity of the peak from 212 cm⁻¹, the displacement of the peak from 272 cm⁻¹ to 287 cm⁻¹, but also the disappearance of the band between 1200- 1400 cm⁻¹, indicates some bonds for Fe-O, FeOOH and Fe (OH)₃, respectively, compounds that can form iron oxyhydroxides that precipitate in solution [45].

The data obtained by Raman spectroscopy are in good correlation with those obtained in FTIR spectra, supporting the presence of reaction products as a result of the interaction of CuFeS₂ samples with organic compounds DFs.

6.1.2. Characterization by Scanning Electron Microscopy (SEM) and Energy dispersive X-ray spectroscopy

Morphological analysis of CuFeS₂ samples obtained on contact with DFs (CuFeS₂-DF1, CuFeS₂-DF2, CuFeS₂-DF3) and, respectively, without DFs (CuFeS₂), was performed by Scanning Electron Microscopy.



SEM images and EDX spectra obtained for samples of CuFeS₂-DF1, CuFeS₂-DF2, CuFeS₂-DF3 and CuFeS₂

All the analyzed samples from the SEM images show non-uniform, flat surfaces, with different morphologies, most likely the result of the process of preparing the surfaces of CuFeS₂ sulfide samples.

A compact structure is observed, which resulted from the agglomeration of primary CuFeS₂ particles dispersed ethanol solution of DFs compounds (DF1, DF2 and DF3, respectively), but also due to the formation of reaction products on the sample surface.

EDX analysis indicates the main elements present on the surface of the analyzed samples: sulfur, iron and copper with some compositional differences, as an effect of the different structure of DFs compounds. The presence of elements, such as silicon and aluminum, respectively, is due to the natural origin, chalcopyrite being often accompanied by other minerals (in this case, most likely with bauxite and quartz).

It is also observed that sulfur is predominant in all samples analyzed, noting that after contact with organic compounds DFs, a slight decrease of the percentage is observed by about $1.7 \pm 1.63\%$ in the order: **CuFeS₂ > CuFeS₂-DF1 > CuFeS₂-DF3 > CuFeS₂-DF2.**

6.3. Inhibition of the oxidation process using DFs

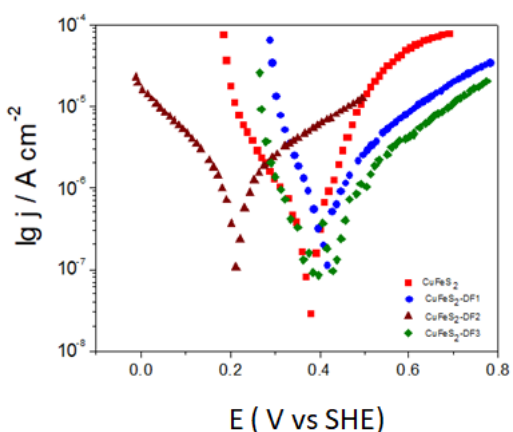
For confirmation, electrochemical studies were performed using Potentiodynamic Polarization (PP) and Electrochemical Impedance Spectroscopy (EIS) techniques.

The electrochemical analysis offers the possibility to evaluate the processes carried out at the mineral surface, by using the CuFeS₂ sample as a working electrode.

To evaluate the inhibitory efficiency of DFs with respect to CuFeS₂ oxidation, samples of CuFeS₂ and DFs were evaluated by electrochemical measurements of PP.

The electrochemical measurements were performed in a three-electrode cell connected to an electrochemical station, Zahner Zanium with Thales analysis program. Methodology for obtaining the working electrode (WL), the carbon paste electrode (CPE).

Potentiodynamic Polarization (PP) curves of CPE electrodes.



CPE-CuFeS ₂	E _{ox} V	j _{ox} nA·cm ⁻²	b _a mV/dec	b _c mV/dec
CuFeS ₂ -DF1	0,403	103	98,3	-66,8
CuFeS ₂ -DF2	0,208	104	22	-153
CuFeS ₂ -DF3	0,369	56,1	153	-74
CuFeS ₂	0,378	84,3	68,7	-102

Polarization Potentiodynamic curves and electrochemical parameters obtained for the CPE electrode, in acidic solutions at pH 2.5 and 25°C

The analysis of the Potentiodynamic Polarization curves shows a shift of the oxidation potential (E_{ox}) towards the cathodic area for the CuFeS₂-DF2 sample.

It is observed that the anodic current densities decrease for the experiments performed on CPE electrodes treated with phenacyl DFs compounds in the order: $CuFeS_2 > CuFeS_2-DF1 > CuFeS_2-DF2 > CuFeS_2-DF3$. On the cathodic area (where the reduction process takes place) the current densities fluctuate around the values obtained on the $CuFeS_2$ sample, untreated with DFs.

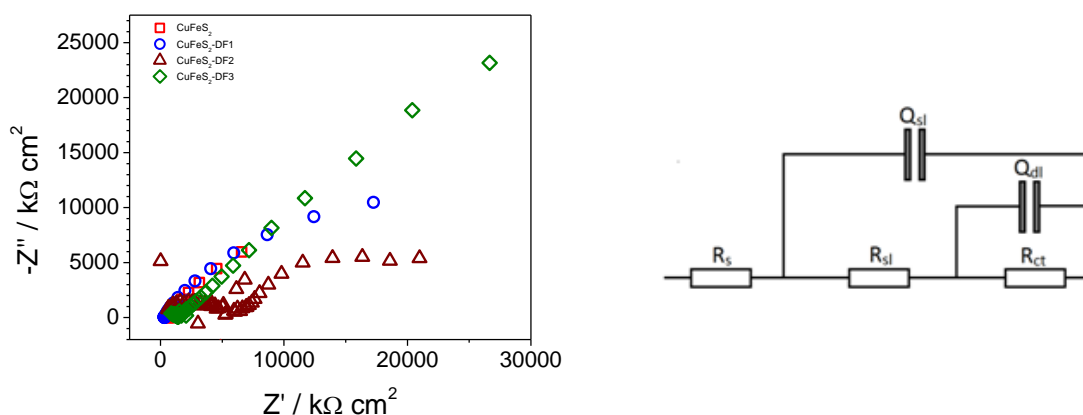
The electrochemical parameters calculated by Tafel analysis highlight the compound DF3 as an anodic inhibitor.

The oxidation current density recorded on the chalcopyrite electrode decreases from $84.3 \text{ nA}\cdot\text{cm}^{-2}$ (in the absence of DFs) to $56.1 \text{ nA}\cdot\text{cm}^{-2}$ for chalcopyrite treated with DF3. The inhibition efficiency was calculated and an inhibition efficiency of 34% was obtained for compound DF3.

From the results obtained by the potentiodynamic polarization of CPE electrodes in the treatment with DFs compounds and the analysis of electrochemical parameters, it can be concluded that compound DF3 can be considered an effective inhibitor for the surface oxidation reaction of $CuFeS_2$.

CPE electrodes made of $CuFeS_2$ treated with DFs were analyzed by Electrochemical Impedance Spectroscopy, in order to characterize the physicochemical processes at the electrode / solution interface.

The frequency range applied to the samples was set between 100 kHz and 10 mHz, with an amplitude of 10 mV. The data obtained are presented in the form of Nyquist diagrams.



Nyquist diagrams obtained on CPE electrodes, in the treatment with DFs compounds, in acid solutions (pH 2.5), at 25°C and the equivalent electrical circuit used to obtain the impedance parameters

Nyquist diagrams show a single incomplete capacitive loop, which is attributed to the load transfer resistance at the electrode / solution interface [46].

The exception is only at the $CuFeS_2-DF2$ electrode, where two capacitive loops appear on the diagram. These samples show a low frequency capacitive loop (attributed to the charge transfer resistance at the electrode / solution interface) and a high frequency capacitive loop (attributed to the formation of a surface layer formed during sample oxidation).

The experimental results suggest that the oxidation of chalcopyrite in the presence of compounds DF1 and DF3 is controlled by a chemical reaction carried out on the sample surface, while the oxidation process in the presence of compound DF2 is controlled by both a chemical reaction and the diffusion of reactants and / or reaction products on the formed surface layer.

Impedance parameters were obtained by modeling an equivalent electrical circuit.

The impedance parameters obtained on the electrode CPE in acidic solutions (pH 2.5) at 25°C and inhibitory efficiency (η_{Rp})

CPE-CuFeS ₂	R _{sl} Ohm·cm ²	R _{ct} Ohm·cm ²	R _p Ohm·cm ²	η_{Rp} %
CuFeS ₂ -DF1	267	333	600	7,0
CuFeS ₂ -DF2	391	742	1133	51,0
CuFeS ₂ -DF3	392	875	1267	56,0
CuFeS ₂	224	338	562	-

The polarization resistance (R_p) was calculated by summing the surface layer resistance (R_{sl}) and the load transfer resistance (R_{ct}).

From the obtained results it is observed that R_p has an inverse tendency towards that of j_{ox} . An increase in R_p from 562 Ohm·cm² (sample without DFs) to 1267 Ohm·cm² (sample of CuFeS₂-DF3) shows a process of inhibition of the oxidation reaction of chalcopyrite due to the presence in the reaction system of the compound DF3. Compound DF2 records an increase in R_p to 1133 Ohm·cm², but DF1 only 600 Ohm·cm².

Based on the obtained data, the inhibition efficiency was calculated indicating an increase in the order: CuFeS₂ > CuFeS₂-DF1 > CuFeS₂-DF2 > CuFeS₂-DF3.

The maximum standard deviation for the electrochemical impedance parameters is $\pm 1,9\%$. These results, correlated with the results of the electrochemical parameters from the Potentiodynamic Polarization, indicate a superior inhibitory effect of the compound DF3 for the oxidation of CuFeS₂ samples compared to the other phenacyl compounds.

6.2. Characterization of oxidative processes for CuFeS₂ using three Schiff bases grafted with TRIS units

Samples were obtained from natural chalcopyrite and acidic Schiff base solutions grafted with TRIS units (STs) of 1 mM concentration, at pH 2.5 and 25 °C, noted: CuFeS₂-ST1, CuFeS₂-ST2, CuFeS₂-ST3.

Structural analyzes were performed by Raman Spectroscopy and Scanning Electron Microscopy and compositional analysis by Energy dispersive X-ray spectroscopy (EDX).

6.2.1. Structural characterization of samples by Raman Spectroscopy

The representative Raman peaks recorded on CuFeS₂ samples are assigned to spectral ranges between 100-300 cm⁻¹, 400-600 cm⁻¹ and 1200-1400 cm⁻¹, respectively.

The Raman peaks in the spectral ranges between 100-370 cm⁻¹ and 450-600 cm⁻¹ can be attributed to the S-S-S bonds and the S-S bond, respectively.

The spectra of the CuFeS₂-ST2 and CuFeS₂-ST3 samples show a significant decrease in the intensity of the Raman peak from position 461 cm⁻¹ until its complete disappearance (peak attributed to Cu-S bonds), simultaneously with the increase of the relative intensity of the peak at position 289 cm⁻¹, attributed to Fe-S bonds. In the untreated sample spectrum, CuFeS₂ peak intensity at 461 cm⁻¹ is significant.

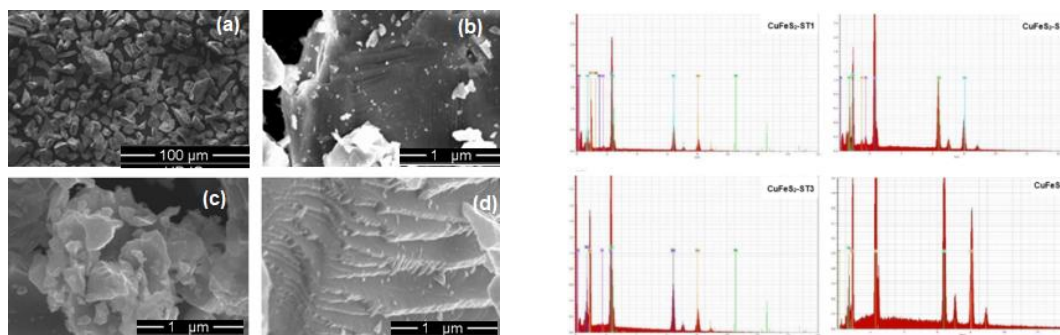
It is a slight shift from the 474 cm⁻¹ position in the spectrum of CuFeS₂-DF1 samples, the position of the peak being attributed to the Cu-S bonds.

A change in intensity, corroborated with the appearance / disappearance of peaks, clearly indicates a chemical interaction of CuFeS₂ with organic compounds of the Schiff base class grafted with TRIS units: ST1, ST2 and ST3.

6.2.2. Characterization by Scanning Electron Microscopy (SEM) and Energy dispersive X-ray spectroscopy

SEM analysis on the $\text{CuFeS}_2\text{-ST1}$ sample indicates the appearance of exposed particles on the flat surface of the sample. The untreated sample of CuFeS_2 analyzed in acid solution (pH 2.5) indicates small structural changes, but the surface is flat and homogeneous.

In the case of $\text{CuFeS}_2\text{-ST2}$ and $\text{CuFeS}_2\text{-ST3}$ samples, agglomerations of particles can be identified that can be attributed to the formation of the surface layer with the new reaction products, which can prevent the transfer of electrons from the mineral structure in solution.



SEM images and EDX spectra at samples $\text{CuFeS}_2\text{-ST1}$ (a), $\text{CuFeS}_2\text{-ST2}$ (b), $\text{CuFeS}_2\text{-ST3}$ (c) and CuFeS_2 (d)

The EDX analysis of the samples of $\text{CuFeS}_2\text{-ST1}$, $\text{CuFeS}_2\text{-ST2}$, $\text{CuFeS}_2\text{-ST3}$ was performed from the images of the SEM analysis, using the same equipment and the aim was to identify the majority of the existing elements on the surface of the samples.

The obtained results highlight as main elements Cu, Fe and S, existing in the structure of chalcopyrite. In the sample treated with the compound ST3 $\text{CuFeS}_2\text{-ST3}$, a decrease in the percentage of sulfur by about 15% and, respectively, an increase in the percentage of iron by about 4%, and for copper by about 8%, indicating a higher interaction between the organic compound and the surface of the metal sulfide.

At the same time, for the samples treated with the organic compound ST1 and the organic compound ST2, respectively, the analysis indicates small differences in the percentage of copper, a slight increase (about + 0.8%) and iron (about + 2%), but a decrease of percentage of sulfur by about 7%, which denotes the formation of a layer of reaction products which does not have a major influence on the oxidative reaction on the surface of the sulfur.

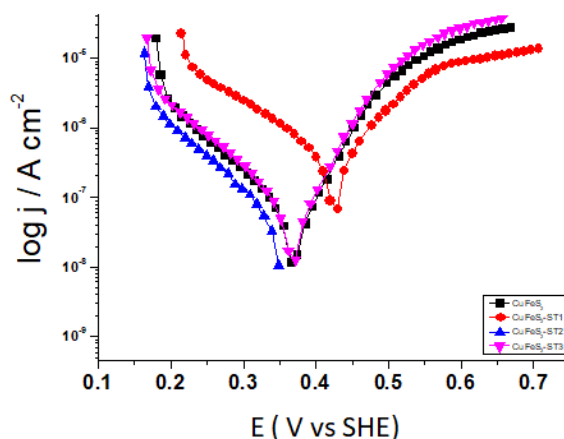
6.3. Inhibition of the oxidation process by electrochemical measurements

Two electrochemical techniques were used: Potentiodynamic Polarization (PP) analysis and Cyclic Voltammetry (CV). The electrochemical experiments were performed in a conventional cell with three electrodes (the reference electrode was the saturated calomel electrode (ECS), the Pt counter electrode and the working electrode in the carbon paste electrode (CPE)) in which they were embedded 0, 02 g of sample to be analyzed.

Electrochemical tests were performed at room temperature, on the CuFeS_2 electrode, in 250 mL acid solution, with the presence of Schiff base compounds grafted with units TRIS, STs (ST1, ST2 and ST3, respectively), pH 2.5 (obtained by dropwise addition of 1 N HCl).

Potentiodynamic Polarization curves indicate a slight decrease in oxidation current density in the presence of the Schiff base grafted with TRIS, ST1 units on both the anodic and

cathodic areas, demonstrating that ST1 can act as a mixed type inhibitor for the reaction oxidation of CuFeS_2 .



Potentiodynamic Polarization obtained on the CPE electrode, in acidic solutions of ST1, ST2 and ST3 at a concentration of 1 mM, at pH 2.5 and 25°C

Data obtained by Potentiodynamic Polarization of CPE in ST3 solutions indicate an approximately constant oxidation potential (E_{ox}). The anodic polarization curves denote a slight increase in the oxidation current density, while the cathodic area remains at approximately constant values.

The electrochemical parameters were extracted by Tafel analysis of the polarization curves and from the values of the oxidation current densities the inhibition efficiency of STs compounds was calculated, for the oxidation reaction of CuFeS_2 .

Electrochemical parameters obtained by Tafel analysis of Potentiodynamic Polarization Curves for the CPE electrode in solutions of ST1, pH 2.5 and 25 °C

CPE	E_{ox} V	j_{ox} $\mu\text{A}\cdot\text{cm}^{-2}$	b_a mV/dec	b_c mV/dec	$\eta_{j_{ox}}$ %
CuFeS_2 - ST1	0,418	180,0	121	-161	54,0
CuFeS_2 - ST2	0,351	97,5	66,7	-97.2	75,0
CuFeS_2 - ST3	0,376	135,0	55,0	-107	66,0
CuFeS_2	0,418	388,0	141	-196	-

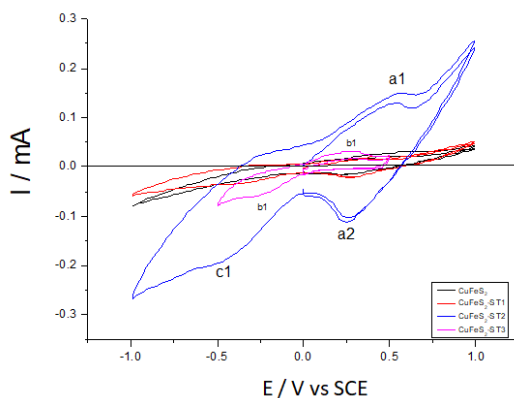
Also, the extracted parameters indicate a maintenance of the oxidation potential (E_{ox}) at 0.418 V, regardless of the reaction medium.

Decreasing the density of the oxidation current (j_{ox}) from 388 $\mu\text{A}\cdot\text{cm}^{-2}$ to 180 $\mu\text{A}\cdot\text{cm}^{-2}$ denotes that ST1 acts as an inhibitor for CuFeS_2 oxidation. The presence of the ST2 inhibitor in acidic solutions has the effect of decreasing the density of the oxidation current (j_{ox}) up to 97.5 $\mu\text{A}\cdot\text{cm}^{-2}$, and the presence of the ST3 compound up to 135.0 $\mu\text{A}\cdot\text{cm}^{-2}$.

The 75% inhibition percentage is due to the N and O atoms, but also to the aromatic nucleus in the ST2 structure which can facilitate the adsorption on the metal surface.

The inhibition efficiency is 54%, recorded in the case of the use of the ST1 compound, which can be associated with the complexity of the adsorption mechanism, and in the case of the ST3 compound, the inhibition efficiency is 66%.

From the recorded voltammograms there are signals that can be attributed to the formation of reaction products, both on the anodic area and at negative potentials. Two positive potentials are observed in the voltammograms of the CuFeS₂-ST2 sample, in which the first peak (a1) at E = 0.56 V / SCE and the second peak (a2) at E = 0.25 V / SCE, can be attributed to the oxidation of the ST2 compound and the formation of CuS compounds and Fe³⁺ ions, and at a negative potential a low is observed at E = -0.47 V / SCE (peak c1) which is attributed to the reduction of sulfur.



Cyclic Voltammograms obtained on the CPE electrode, in acidic solutions of ST1, ST2 and ST3, at pH 2.5 and 25°C

The voltammogram obtained on the electrode of the CuFeS₂-DF3 sample shows the presence of a peak marked with b1 at E = -0.25 V / SCE and, respectively, the peak b2 at E = 0.27 V / SCE, positions that can be associated, according to the literature, the oxidation of Fe²⁺ ions to Fe³⁺ and their reduction, respectively.

7. Synthesis and characterization of ZnS nanoparticles using capture agents

This chapter presents the synthesis of ZnS nanoparticles using two new organic capture agents (a new Schiff base and a new phenacyl derivative), aiming to stop the growth of nanoparticles, in order to detect and degrade toxic pollutants of heavy metal ions resulting from MeS oxidation.

A simple method of chemical co-precipitation is used to synthesize the cubic phase of ZnS nanoparticles [47-51]. Both the phenacyl derivative (DF) and the TRIS (hydroxymethyl) aminomethane (TRIS) are structural units of importance in biochemistry and molecular biology [52,53]. The structure, morphology and optical properties of ZnS NPs prepared with / without capture agents will be analyzed using methods such as: XRD, SEM / EDX and UV-vis.

7.1. Synthesis of the ZnS NPs

7.1.1. Materials

Precursors were used: hydrated zinc acetate (C₄H₆O₄Zn·2H₂O) and sodium sulfide (Na₂S), chemicals purchased from Merck.

The phenacyl derivative (DF), 4-Phenyl-2-N-morpholinyl-thiazole (C₁₃H₁₄N₂OS, M=246 g/mol) and the Schiff base grafted with TRIS units (TRIS) (C₄H₁₁NO₃, M =121 g/mol).

These two organic compounds have been studied as organic inhibitors for the oxidation process at MeS.

The chosen phenacyl derivative has the most stable structure with ZnS, the anchoring on the sulfide surface being achieved by means of Zn atoms (2).

The Schiff base grafted with TRIS units was studied for the oxidation process at PbS and CuFeS₂, respectively, registering inhibition efficiencies of over 60% for the oxidative processes of these minerals.

The synthesis of ZnS nanoparticles (Zns NPs) with and without capture agents was performed in aqueous medium, where the capture agent was added, dissolved in absolute ethyl alcohol (99.9%).

7.1.2. Synthesis reaction in obtaining ZnS NPs

Solutions of zinc acetate (25 mM) and sodium sulfide (25 mM) were prepared, the samples being magnetically stirred (2000 rpm) for 30 minutes at a temperature of 65°C. Solutions of capture agents, DF and TRIS in ethyl alcohol (25 mM) were prepared.

In a first step, 10 mL of organic compound solution (DF or TRIS) was added dropwise to the zinc acetate solution (25 mL) to avoid agglomeration of the precipitated ZnS particles.

Immediately, 25 mL of sodium sulfide was added dropwise, and a white-yellow precipitate was observed for the synthesis of ZnS nanoparticles with the phenacyl derivative DF, and a white precipitate for the synthesis of ZnS nanoparticles with Schiff base grafted with TRIS units.

ZnS samples were synthesized without the addition of organic compound, following the same procedure, resulting in a white precipitate.

The resulting precipitates were separated by decantation, washed with Et-OH (99.9%) and dried in an oven at 80°C for 6 hours. The synthesis yield was 58% for ZnS NPs, 64% for ZnS NPs-TRIS and 69% for ZnS NPs-DF, respectively.

The resulting powders were emptied into specific containers (TEFAL Plus VT256070) and used for structural and functional characterization.

7.2. Structural and spectrochemical characterization of ZnS nanoparticles, using TRIS and DF as capture agents

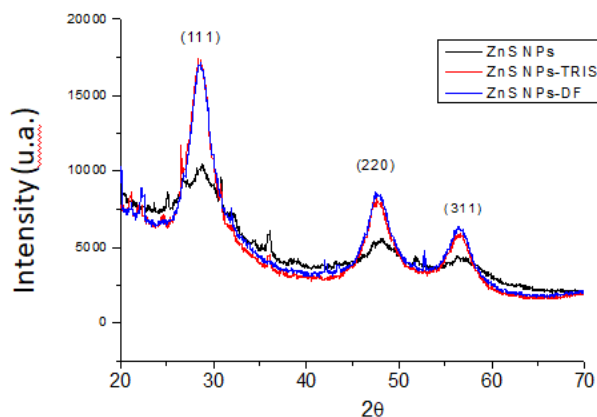
Samples of ZnS nanoparticles were characterized by modern methods of analysis.

- X-ray diffraction (XRD) is the method used to confirm the structure of newly synthesized materials (ZnS NPs) and calculate the size of ZnS NPs crystals (Scherrer equation). XRD measurements were performed at room temperature with a monochromatic CuK α radiation, with a wavelength of 1.54059 Å. The Rigaku Smart Lab diffractometer (Applied Sciences Research Center -INCESA-Craiova) was used.
- Fourier transform infrared spectroscopy (FTIR) is useful for investigating the phases on the surface of ZnS NPs, with and without the capture agent (ZnS NPs-DF and ZnS NPs-TRIS). The spectra were recorded over a wavelength range from 200 to 4000 cm⁻¹, using a resolution of 2 cm⁻¹, using as a technique the determination with probe included in the equipment - (Bruker Alpha, Faculty of Sciences, University of Craiova).
- Scanning electron microscopy (SEM) is useful for obtaining SEM images for ZnS NPs. Energy dispersive X-ray spectroscopy will identify the major elements in the composition of ZnS NPs (Philips XL 30 FEG Electronic Microscope - University of Lower Danube, Galați).
- UV-vis spectrophotometry is a method that offers the possibility to investigate the optical properties of nanomaterials, without modifying or damaging their properties. From the synthesized samples (ZnS NPs, ZnS NPs-DF and ZnS NPs-TRIS) dispersions (10 mL) were

obtained with a concentration of 1 mM, analyzed over a wavelength range from 200 to 1200 nm, at room, using a quartz tub, 1 mL (UV-vis spectrophotometer PG Instruments - Faculty of Sciences, University of Craiova).

7.3. X-ray diffraction (XRD)

The obtaining of ZnS nanoparticles (ZnS NPs) is confirmed by the observed peaks at values of angles of 2θ such as: 33° , $47,4^\circ$, $56,4^\circ$ and $69,4^\circ$ that match the planes (111), (220), (311) and (400), respectively, the crystalline planes corresponding to the face-centered cubic structure for pure ZnS [51-54].



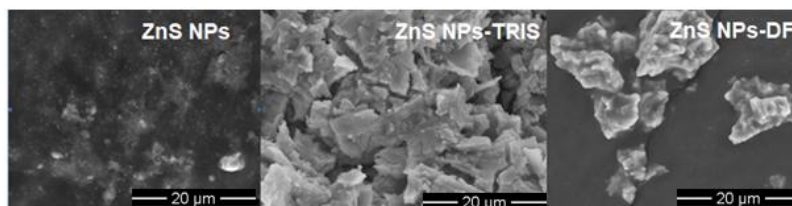
XRD spectra at ZnS NPs compared to ZnS NPs-TRIS and ZnS NPs-DF

The crystal size calculated with the Scherrer's equation was: ZnS NPs = 8.57 ± 1 nm, ZnS NPs-TRIS = 4.28 ± 1 nm and ZnS NPs-DF = 4.28 ± 1 nm, thus indicating an inhibition of nanoparticles agglomeration obtained by about 50%.

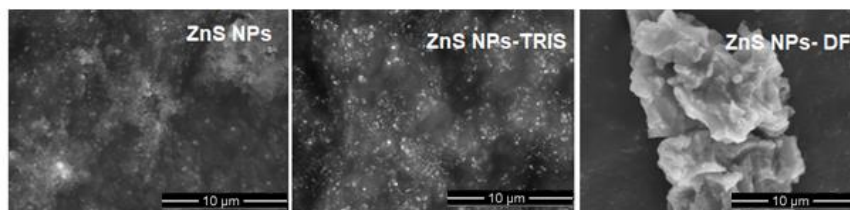
7.4. Structural Characterization by Scanning Electron Microscopy (SEM)

The morphology of ZnS nanoparticles was analyzed by SEM, the images being presented at dimensions of $20 \mu\text{m}$, dimensions of $10 \mu\text{m}$, dimensions of $5 \mu\text{m}$ and dimensions of $2 \mu\text{m}$. In the absence of a capture agent, ZnS NPs appear with distribution over the entire surface in agglomerated form. Stabilization, in case of TRIS use in the synthesis process and limitation of agglomeration process, in case of DF use, is highlighted after the use of the capture agent in the synthesis process (ZnS NPs-TRIS and ZnS NPs-DF).

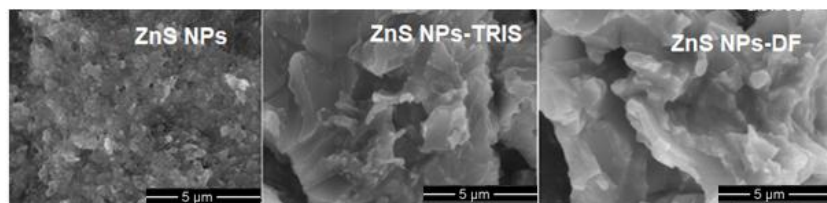
Changes in the morphological and optical properties of the obtained ZnS nanoparticles were observed by changing the capture agent.



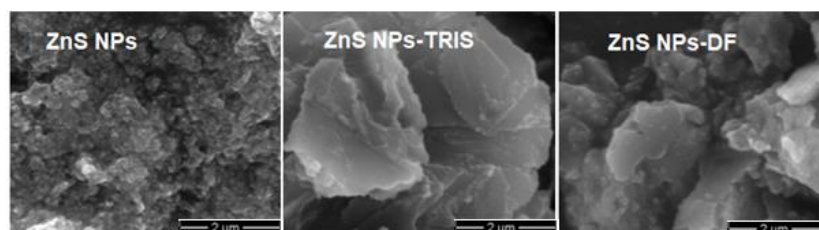
SEM images for ZnS NPs compared to ZnS NPs-TRIS and ZnS NPs-DF, at dimensions of $20 \mu\text{m}$



SEM images for ZnS NPs compared to ZnS NPs-TRIS and ZnS NPs-DF, at dimensions of 10 μm



SEM images for ZnS NPs compared to ZnS NPs-TRIS and ZnS NPs-DF, at dimensions of 5 μm



SEM images for ZnS NPs compared to ZnS NPs-TRIS and ZnS NPs-DF, at dimensions of 2 μm

SEM microstructural analysis shows that synthesized ZnS NPs contain mainly regular-shaped ZnS particle granules. Nanoparticles with almost spherical shapes have a homogeneous distribution, having different average sizes, such as: ZnS NPs $d_{med} = 32.5 \text{ nm} \pm 2 \text{ nm}$, ZnS NPs-TRIS $d_{med} = 39 \text{ nm} \pm 2 \text{ nm}$ and ZnS NPs-DF $d_{med} = 36.1 \text{ nm} \pm 2 \text{ nm}$.

An increase in crystallite size is explained by the absorption of the capture agent on the surface of ZnS nanoparticles, also confirmed by EDX analysis.

7.5. Elemental analysis by Energy dispersive X-ray spectroscopy (EDX)

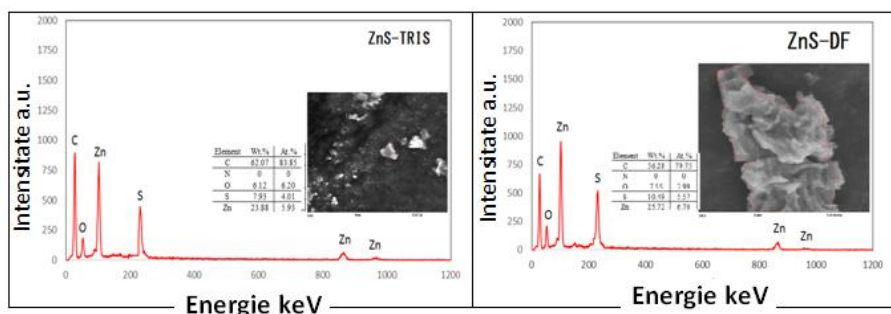
The elemental composition of the synthesized nanoparticles was confirmed by Energy dispersive X-ray spectroscopy (EDX), performed on SEM images. The composition of the samples analyzed by EDX analysis confirms elements (Zn and S) of ZnS NPs, with low content and the presence of carbon on nanoparticles obtained with capture agents. Oxygen is present in the analysis, on the ZnS NPs sample, its percentage decreasing considerably for the samples with capture agents (ZnS NPs-TRIS and ZnS NPs-DF).

The analysis on images confirms for C, S and O a 50% reduction for the content of all elements, compared to the sample without capture agent.

*EDX analysis for ZnS NPs
compared to ZnS NPs-TRIS and ZnS NPs-DF*

Samples	Zn (%)	S (%)	O (%)	C (%)
ZnS NPs	55,60	26,30	18,10	-
ZnS NPs- TRIS	23,88	7,93	6,12	62,07
ZnS NPs- DF	25,72	10,49	7,55	56,28

Therefore, there is no difference in elemental content for samples where TRIS or DF capture agents were used in the synthesis of ZnS NPs.

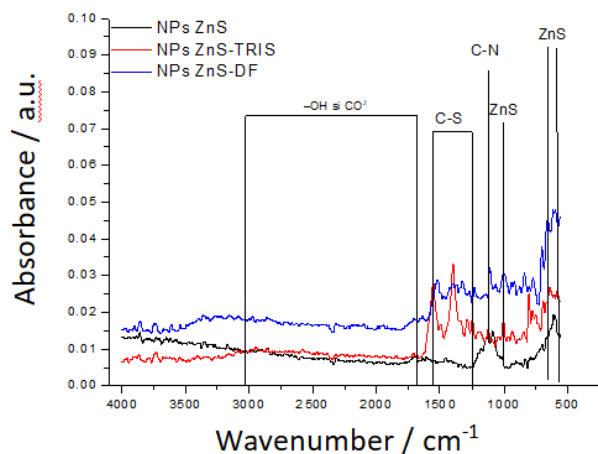


EDX analysis for ZnS NPs-TRIS and ZnS NPs-DF

EDX analysis confirms the presence of organic compounds in the analyzed samples, between the two capture agents there being no major differences in the compositional map, but it presents a different distribution for ZnS NPs-TRIS and ZnS NPs-DF.

7.6. Structural Characterization by Fourier Transform Infrared Spectroscopy (FTIR)

The FTIR spectra for ZnS NPs without capture agent, and respectively, using capture agents (ZnS NPs-TRIS and ZnS NPs-DF) show differential peaks that can be successfully attributed to ZnS NPs capture. The appearance of peaks at 563 cm^{-1} , 653 cm^{-1} , 1009 cm^{-1} confirms the formation of ZnS NPs [55-56].



FTIR spectra for ZnS NPs compared to ZnS NPs-TRIS and ZnS NPs-DF

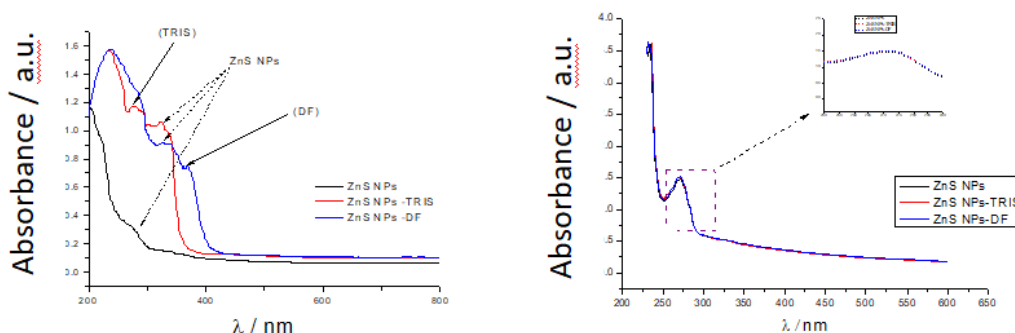
The presence of capture agents on the surface of nanoparticles can be represented by the CN (1108 cm^{-1}) C=C (1641 cm^{-1}), C-O (1248 cm^{-1}) bonds highlighted in the spectrum showing the capture of ZnS NPs with the capture agent DF. Peaks at $1242\text{--}1552\text{ cm}^{-1}$ are associated with C-S type intramolecular binding.

For ZnS NPs-TRIS the bond of the organic compound with ZnS is rendered by S atoms. The peaks at $1637\text{--}3434\text{ cm}^{-1}$ confirm the presence of CO_2 and H_2O adsorbed on the surface of ZnS NPs [56].

These peaks confirm the link between the organic compound used as a capture agent and the ZnS nanoparticles.

7.7. Spectral properties specific to ZnS nanoparticles

Dispersions of ZnS NPs, 10^{-3} M concentration, were performed, and UV-vis analysis was performed over a wavelength range of $200\text{--}800\text{ nm}$.



UV-vis spectra, initially and after 30 days, for the dispersion of ZnS NPs compared to ZnS NPs-TRIS and ZnS NPs-DF, at 10^{-3} M and 25°C

The appearance of the peak at λ of 323 nm indicates the formation of ZnS nanoparticles [52,55]. After capture of ZnS NPs, with the capture agents DF (ZnS NPs-DF) and TRIS (ZnS NPs-TRIS), respectively, the formation of peaks can be observed in the same wavelength

range (323 nm), but with different adsorption (for ZnS NPs-TRIS the adsorption is 1.063 au and for ZnS NPs-DF the adsorption is 0.910 a.u.), due to the different structure of the organic compound and the improvement of the optical properties.

The appearance of the peaks highlighted in the range of 300–330 nm in the spectra obtained for ZnS NPs-DF and ZnS NPs-TRIS has a characteristic of the higher absorption band compared to the uncaptured nanoparticles.

The dispersions obtained, dispersion of ZnS NPs, ZnS NPs-TRIS and ZnS NPs-DF (10^{-3} M), kept in hermetically sealed containers, were analyzed after 30 days, by dilutions to 10^{-6} M, over a length range wavelength from 200 nm to 650 nm.

The spectrum profile does not indicate major differences and confirms a uniform stability of the solutions over time. There is only one peak, at a wavelength of 265 nm, which can be associated with the stabilization of ZnS nanoparticles over time, being a change of 60 nm (hispochromic effect), the nanoparticles becoming smaller. The recorded absorbance differs (1,506 u.a. for ZnS NPs-DF, 1.4738 u.a. for ZnS NPs-TRIS, compared to 1.3577 u.a. for ZnS NPs), indicates an improvement of the optical (photocatalytic) properties of the nanoparticles, by using organic compounds such as capture agents.

Optical band values (E_g) were calculated. For ZnS NPs $E_g = 3.71$ eV, and for ZnS NPs-TRIS and ZnS NPs-DF, $E_g = 3.83$ eV. These values confirmed an improvement in E_g by the use of the capture agent in the synthesis of ZnS NPs.

The pH and conductivity (λ) of the ZnS NPs solutions were analyzed with the two capture agents (1 mM) in the aqueous medium at 25°C (CONSORT C3021). The samples were initially analyzed, then placed in airtight containers and analyzed 3 and 6 days after preparation.

The pH and conductivity values (λ) for dispersions of ZnS NPs (1 mM), obtained with DF and TRIS capture agents, at 25°C

Time (days)	ZnS NPs		ZnS NPs-DF		ZnS NPs-TRIS	
	pH	λ (μ S/cm)	pH	λ (μ S/cm)	pH	λ (μ S/cm)
0	6,22	1047	5,91	1163	5,56	1156
3	6,80	1229	6,00	1325	4,61	1365
6	5,73	1333	6,23	1208	5,82	1385

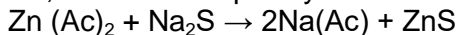
The pH values decreased slowly after the addition of the capture agents to the ZnS NPs synthesis, from pH 6.22 to the nanoparticles without the capture agent to pH 5.56, when DF was used, and at pH 5, respectively, 91 with the use of TRIS. The pH increases after three days for ZnS nanoparticles by +0.58 compared to +0.09 pH units, at ZnS-TRIS, which even after 6 days indicates an increase of +0.23. For ZnS NPs-DF a decrease of about one unit pH after 3 days and then a slight increase.

The increase in conductivity from 1047 μ S/cm (ZnS NPs) to 1370 μ S/cm (ZnS NPs - DF) and 1156 μ S/cm (ZnS NPs-TRIS), respectively, is due to the conductive nature of charged ZnS nanoparticles, dispersed in solution. These changes indicate an improvement in the electrical properties of ZnS NPs, using DF and TRIS capture agents in synthesis.

After 3 days there is an increase in conductivity in the case of ZnS NPs-TRIS, from 1229 μ S/cm to 1365 μ S/cm and from 1333 μ S/cm to 1385 μ S/cm, respectively, for a reaction period of 6 days, which indicates a good efficiency of electric charge transport, but also a good stability in time for the obtained samples.

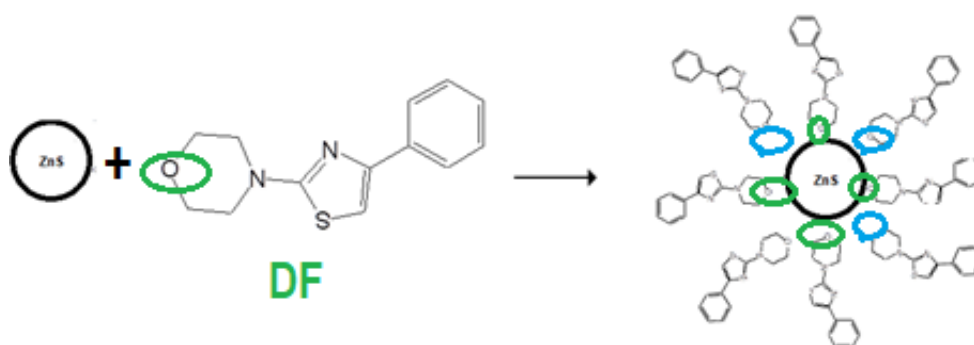
7.8. The synthesis mechanism

The precursors were: zinc acetate and sodium sulfide, which dissociated into cations (Zn^{2+} , Na^{2+}) and anions (CH_3COO^- , S^{2-}). Sodium ions easily form sodium acetate, with sodium being more reactive than zinc. ZnS particles are formed due to the reaction between zinc and sulfur ions, which subsequently increase by consuming ions in solution.



The growth of ZnS nanoparticles can be limited, either by the accumulation on the surface of Na^{2+} ions (from the Na_2S solution), or by the introduction into the reaction system of a capture agent, an organic compound.

There is a possible mechanism for capturing ZnS NPs with DF, adapted from the literature, the binding of the organic compound to ZnS NPs can be considered by means of oxygen ions.



Proposed mechanism for capture with DF in synthesis ZnS nanoparticles

Conclusions

Environmental pollution due to mining activities is a serious source of release of high concentrations of heavy metals, whose presence is due to polluting waters mainly by oxidation of metal sulfides (MeS) from the earth's crust and are brought to the surface by mining activities.

Methods to inhibit the oxidation of metal sulphides would reduce the polluting impact on the environment (both for the natural environment and for the health of living organisms) and lead to more efficient mining.

In this context, the doctoral thesis had as main objective the study of the efficiency of some organic inhibitors to the oxidative processes of metal sulfides.

The paper includes in the documentary part, information on the oxidation processes of some MeS, the impact for the environment, but also methods for their inhibition. It was found that the oxidation of MeS develops according to the mechanism of metal corrosion, thus offering the chance to investigate some chemicals with the role of inhibitors.

The main scientific contribution of the paper aims to identify effective inhibitors for the oxidation process of the most reactive metal sulfides, sphalerite (ZnS), troilite (FeS), chalcopyrite (CuFeS_2) and galena (PbS), using as inhibitors, synthesized organic compounds which offer the possibility to model the "support" structure by adding heteroatoms or aromatic nuclei, which can make inhibition more efficient.

To investigate the oxidative process in MeS, natural metal sulfides of sphalerite (ZnS), galena (PbS), chalcopyrite (CuFeS_2) and, respectively, a synthetic metal sulfide, troilite (FeS)

(purchased from Merck), the basic structures of sulfides being confirmed by X-ray diffraction analysis (XRD).

Studies have been initiated to inhibit the oxidation of these sulfides using two types of organic molecules, newly synthesized structures, from the class of phenacyl-derived compounds (DFs) and Schiff bases grafted with TRIS units (STs), and an aminoacid, glycine, purchased by at Merck).

The phenacyl derivatives (DFs) studied were: 1-(3,5-dibromo-2-hydroxyphenyl) -1-oxoethane-2-yl-phenyl-2-N-morpholinyl-thiazole (DF1), N,N-diethyldithiocarbamate -yl (DF2) and 1-(5-bromo-2-hydroxy-3-methylphenyl)-1-oxoethan-2-yl (DF3) O-Ethylxantogenate.

These compounds have in their structure an aromatic nucleus and an OH group, and also a chain of 2 carbon atoms to which heteroatoms of N and O bind. The structural differences are as follows: on the structure of the compound DF1, by supplementation with two atoms of N and an atom of S, on the structure of the compound DF2, by adding two S atoms, one of N, two Et-OH groups and two Br atoms and, respectively, on the structure of the compound DF3 by adding an Et-OH group and two S atoms.

It is believed that the molecules of compounds DF1 and DF3 will act as effective inhibitors for the oxidation reaction to MeS, because they have successive heteroatoms (S, N, O, Br) at "anchoring" on the metal surface. In the case of the molecule of the compound DF2, although it has such atoms, its molecular structure is more complex, which would induce a complex reaction mechanism, thus leading to lower inhibition efficiencies compared to DF1 and DF3.

Phenacyl-derived compounds are used in the scientific approach to inhibit the oxidation of natural samples of ZnS (Chapter 3) and CuFeS₂ (Chapter 6).

Schiff bases grafted with TRIS units (STs) have the chemical formulas: C₂₀H₃₂N₂O₇ (ST1), C₁₁H₂₁NO₄ (ST2) and C₄H₁₁NO₃ (ST3) and have as a structure a chain of four carbon atoms to which one nitrogen atom and three oxygen atoms bind .

Structural differences consist in, the presence of an aromatic nucleus for the structure of compound ST1 and compound ST2 and, respectively, different number of N and O atoms, highlighted in the structure of compound ST3, by supplementation with an N atom and 3 O atoms, in the structure compound ST2, by supplementation with one N atom and 4 O atoms, and for compound ST1 by supplementation with 2 N atoms and 7 O atoms.

In this case, the differentiated structures are expected to increase the inhibition efficiency of metal sulfides, but the complexity of the reaction mechanism that may make it difficult to bind them to the metal surface must also be considered.

These compounds are used for the oxidation of natural samples of PbS (Chapter 5) and CuFeS₂ (Chapter 6), and for synthetic FeS samples only the ST1 molecule was studied (Chapter 4).

The research began by performing quantum calculations (using the Amsterdam Functional Density (ADF) program), the results contributing to a good understanding of the processes and mechanisms of inhibition for metal sulfide oxidation (MeS).

To begin with, by quantum modeling, for the molecules of the analyzed compounds (DFs, STs and glycine), the boundary molecular orbitals were obtained (the molecular orbital occupied with the highest energy level (HOMO), the molecular orbital occupied with the lowest level), (LUMO)), in order to identify the centers capable of connecting to the metal surface.

For the analyzed compounds, quantum parameters were obtained by calculation (dipole moment (μ), energy of the molecular orbital occupied with the highest energy level (E_{HOMO}), energy of the unoccupied molecular orbital with the lowest energy level (E_{LUMO}) and the energy band ($\Delta E = E_{\text{LUMO}} - E_{\text{HOMO}}$)), all these parameters helping to a better knowledge of the adsorption mechanism of organic matter, on the tested metal surface.

The MeS surface was modeled and from the multitude of offering surfaces, a case study was chosen, using a cluster derived from the MeS surface.

The geometries of the adsorption structures for the tested compounds (DFs and STs) were modeled on the cluster derived from the MeS surface and the adsorption energies (E_{ad}) of the compounds on its surface were calculated. Thus, by quantum analysis, the most relevant solutions for inhibiting the oxidative process for MeS were identified, but also which organic compounds would be more efficient in the oxidative process.

Samples were obtained by treating the metal sulfides with the analyzed organic compounds (all solutions of organic compound having a concentration of 1 mM), in an acidic pH medium (pH 2.5) and at a temperature of 25°C, suitable conditions for the oxidation process. of these materials.

Depending on the solubility of the test compounds, samples of zinc sulfide with phenacyl derivatives (ZnS-DFs) in the alcoholic medium, iron monosulfide with glycine (FeS-gli) in the aqueous medium, lead sulfide with Schiff bases grafted with TRIS units (PbS-STs) in aqueous medium, chalcopyrite with phenacyl derivatives (CuFeS₂-DFs) in alcohol and chalcopyrite with Schiff bases grafted with TRIS units (CuFeS₂-STs) in aqueous medium.

The samples obtained were structurally characterized by modern analysis techniques, Scanning Electron Microscopy (SEM), Fourier Transform Infrared Spectroscopy (FTIR), Raman and Compositional Spectroscopy by Energy dispersive X-ray spectroscopy (EDX).

The impact of organic compounds (phenacyl derivatives, Schiff bases grafted with TRIS and glycine units) in the process of inhibiting metal sulfide oxidation was studied by electrochemical methods, Potentiodynamic Polarization (PP), Cyclic Voltammetry (CV) and Electrochemical Impedance Spectroscopy .

Impact studies of organic compounds on metal sulphides were performed in an aqueous medium of pH 2.5, at 25°C, using, depending on the sulfide analyzed, solid electrodes (for the study of FeS oxidation) and, respectively, carbon paste electrodes (CPE), for the study of ZnS, PbS and CuFeS₂ oxidation.

To investigate the oxidation of FeS samples with glycine and compound ST1 (Chapter 4), PbS with STs (Chapter 5) and CuFeS₂ with STs (Chapter 6.2), electrochemical techniques were performed in aqueous solutions of organic compound, and to inhibit oxidation of samples of ZnS (Chapter 3) and CuFeS₂ (Chapter 6.1) using phenacyl derivatives (DFs). The investigation methodology consisted in pre-treating the samples with organic compounds in alcoholic solutions of 1 mM concentration, and then investigating them in aqueous solutions of pH 2.5, at 25°C.

➤ **From the study performed on the evaluation of the inhibition of the oxidative process of ZnS using phenacyl derivatives, DFs (chapter 3), the following can be noticed:**

- Quantum parameters and modeled structures have indicated that the adsorption of DFs compounds on the mineral surface is achieved by Zn atoms.
- The structural characterization of the obtained samples (ZnS-DF1, ZnS-DF2 and ZnS-DF3) indicates on the reacted surface, the presence of reaction products, which can be associated with a ZnS oxidation inhibition effect.
- Electrochemical parameters obtained by Tafel analysis (PP method) indicated a decrease in oxidation current density (j_{ox}) from 277 nA·cm⁻² (in the absence of DFs) to 3.84 nA·cm⁻² (for ZnS -DF3) and, respectively, the increase of the polarization resistance (R_p) from 157 Ω·cm² (in the absence of DFs) to 8940 Ω·cm² (for ZnS-DF3), thus demonstrating maximum efficiency for the treatment with DF3.
- Inhibition efficiency was calculated from j_{ox} ($\eta_{j_{ox}}$) and polarization resistance R_p (η_{R_p}), respectively, and the results indicated an improvement in inhibition efficiency in the order: ZnS > ZnS-DF2 (71%) > ZnS-DF1 (87 %) > ZnS-DF3 (98%).

- Thus, compound DF3 indicates maximum inhibition efficiency, and compound DF2 has the lowest inhibition efficiency for the oxidation process to ZnS, these results being supported by quantum data.
- Turbidimetric analysis of the concentration $[\text{SO}_4^{2-}]$ of the samples of ZnS-DF1, ZnS-DF2 and ZnS-DF3, in contact for 8 days, with acid solution pH of 2.5 and at 25°C, indicated that the study method it is not a conclusive analysis of the inhibitory effect of the studied organic compounds.

➤ **From the study on the evaluation of the inhibition of the oxidative process of FeS using glycine and a new Schiff base grafted with TRIS units (ST1) (chapter 4), the following can be noticed:**

- The results obtained by quantum analysis for glycine indicate a low value of the dipole moment ($\mu = 0.714$ / Debye), which suggests a moderate interaction between glycine and the FeS surface, but the low value of the energy band ($\Delta E = -3,593$ eV) highlights a good inhibitory effect on the sulfide surface.
- The action of Fe^{2+} and Fe^{3+} ions, from the spectrophotometric analysis, on the mode of glycine adsorption on the surface of the FeS structure indicated that it can bind to the FeS surface via Fe^{3+} ions.
- Corroborating these data with the data obtained by quantum calculations, it can be stated that the adsorption of glycine on the FeS surface is done by HOMO orbitals of glycine and Fe^{3+} ions resulting from the oxidation of the mineral surface. Electrochemical assays of PP and EIS analysis indicated that glycine acts as a mixed type inhibitor for FeS surface oxidation.
- The density of the oxidation current (j_{ox}) increases for a low glycine concentration, from $60.2 \mu\text{A}\cdot\text{cm}^{-2}$ (in the absence of glycine) to $89.2 \mu\text{A}\cdot\text{cm}^{-2}$ ($[\text{glycine}] = 0.02$ mM) , and at a subsequent increase in concentration, for another experiment, a successive decrease of j_{ox} is observed from $66.0 \mu\text{A}\cdot\text{cm}^{-2}$ to $38.7 \mu\text{A}\cdot\text{cm}^{-2}$ ($[\text{glycine}] = 0.50$ mM) , indicating an inhibitory efficiency ($\eta_{j_{\text{ox}}}$) of 41.1%.
- Nyquist diagrams (EIS method) indicate the appearance of the reaction products by the presence of the two capacitive loops: incomplete capacitive loop and complete capacitive semicircular loop. Impedance parameters were extracted by modeling an equivalent electrical circuit and it was observed that the polarization resistance (R_p) increases from $701 \text{ Ohm}\cdot\text{cm}^2$ in the absence of glycine to $1132 \text{ Ohm}\cdot\text{cm}^2$ $[\text{glycine}] = 0.10$ mM, followed by a successive decrease to $688 \text{ Ohm}\cdot\text{cm}^2$ $[\text{glycine}] = 1.00$ mM, indicating an inhibitory efficiency (η_{R_p}) of 38.1%.
- Quantum analysis for the Schiff base grafted with TRIS units (ST1), indicates a good inhibitory effect due to the low value of the energy band ($\Delta E = 0.08$ eV), but the adsorption mechanism is complex and the extension of the two boundary molecular orbitals (HOMO and LUMO) is relatively low, the inhibition process will be moderate for the sulfide surface.
- The electrochemical parameters from the PP analysis, obtained on the FeS electrode in acidic Schiff base solutions grafted with TRIS units, at pH of 2.5 showed a mixed inhibition process. The density of the oxidation current (j_{ox}) decreases from $61.2 \mu\text{A}\cdot\text{cm}^{-2}$ (in the absence of ST1) to $34.1 \mu\text{A}\cdot\text{cm}^{-2}$ ($[\text{ST1}] = 0.52$ mM) with an inhibition efficiency ($\eta_{j_{\text{ox}}}$) of 44.3%.
- Cyclic voltammograms, for acidic solutions of STs, indicate that at the applied positive potential the oxidation process of S (-II) to S (0) and S (+VI) takes place ($E = +0.14/+ 0,03$ V / SCE) and Fe (II) to Fe (III), respectively ($E = + 0.77$ V /SCE).
- Structural characterization of FeS electrodes, performed by Optical Microscopy (MO), before and after electrochemical experiments shows, in both cases, the absence of

traces of physical treatment applied to the electrode for cleaning and the appearance of areas with chromatic differences, which we can associate with formation of reaction products responsible for the inhibition process.

➤ **From the study performed on the evaluation of the inhibition of the oxidative process of PbS using three Schiff bases grafted with TRIS units (STs) (chapter 5), the following can be noticed:**

- Samples obtained with Schiff bases grafted with TRIS STs units (PbS-ST1, PbS-ST2 and PbS-ST3), compared to PbS without STs, confirm in the Raman spectra peaks certifying the Pb-S bonds in the samples.
- SEM images highlight the presence of surfaces with different structural morphologies, with homogeneity, but with dimensions smaller or larger than 1 μm , of the present formations.
- The EDX analysis confirmed that most of the elements present on the sample surfaces are lead and sulfur from the natural sample.
- The PP analysis indicates a mixed inhibition process for the oxidative process of PbS samples, in the presence of STs compounds. Tafel parameters (PP analysis) show compound ST3 having the best inhibition yield, higher than 92%, compound ST2 with inhibition higher than 75%, and compound ST1, the lowest inhibition yield, of 40%.

➤ **From the study performed on the evaluation of the inhibition of the oxidative process of CuFeS₂ using phenacyl derivatives (DFs) and three Schiff bases grafted with TRIS units (STs) (chapter 6), the following can be noticed:**

- Samples were obtained from natural chalcopyrite with phenacyl-derived compounds DFs: denoted CuFeS₂-DF1, CuFeS₂-DF2, CuFeS₂-DF3 and, respectively, with Schiff bases grafted with TRIS STs units: denoted CuFeS₂-ST1, Cu₂FeS₂-ST2, CuFeS₂-ST3.
- For chalcopyrite, quantum analysis indicates for the phenacyl derivative DF3 the most effective inhibition by binding to the surface of the sulfide sample, via the Fe atom.
- Raman and FTIR spectroscopy showed peaks associated with the formation of the reaction products (elemental sulfur, disulfides and polysulphides, iron oxides), responsible for the formation of the surface layer of the samples, through which the oxidation reaction of CuFeS₂ is inhibited
- SEM structural analysis in CuFeS₂ samples with DFs showed uneven surfaces, with different morphologies, which depend on the structure of the organic inhibitor.
- In the treated samples, the predominant elements highlighted by EDX analysis are Cu, Fe and S, with small compositional differences due to the different structure of the organic compounds.
- The electrochemical parameters, from the PP analysis, indicate a decrease in the density of the oxidation current, for example from 84.3 $\text{nA}\cdot\text{cm}^{-2}$ (in the absence of DF3) to 56.1 $\text{nA}\cdot\text{cm}^{-2}$ in the presence of DF3.
- Electrochemical results indicate the compound DF3 as the most effective inhibitor for oxidation of chalcopyrite, with an inhibitory efficiency of 34%.
- Monitoring the evolution of $[\text{Fe}_{\text{tot}}]$ and pH, during 63 days of reaction of CuFeS₂ samples treated with DFs, in acidic solutions, pH 2.5, at room temperature, showed an increase in values $[\text{Fe}_{\text{tot}}]$, and the pH of the solution, respectively, which may indicate an effective inhibitory effect on the oxidation process of CuFeS₂ samples using DFs.
- Structural characterization by SEM analysis for CuFeS₂ samples with STs, indicates inhomogeneous surfaces, which show agglomerations of particles that may be associated with the formation of new reaction products.

- EDX analysis confirms that the major elements are copper, iron and sulfur, in the composition of the samples, and small changes associated with the formation of a thin layer of reaction products on the surface of sulfur, due to the action of STs compounds.
- The electrochemical parameters, from the Tafel analysis (PP method) indicate a decrease of the oxidation current density (j_{ox}) from $388 \mu A \cdot cm^{-2}$ (in the absence of STs) to $180 \mu A \cdot cm^{-2}$ for the compound ST1, to $97.5 \mu A \cdot cm^{-2}$ for compound ST2, and for compound ST3 at $135.0 \mu A \cdot cm^{-2}$.
- The calculated inhibition efficiency indicates a yield of 75% for samples analyzed with compound ST2, 66% for samples analyzed with compound ST3 and 54% for samples with compound ST1, respectively.
- In conclusion, for the oxidative process to $CuFeS_2$ there is a better inhibition efficiency with STs compounds, compared to phenacyl DFs derivatives, with a yield difference of about 27%.

Chapter 7 of the doctoral dissertation presents the synthesis and characterization of zinc sulfide nanoparticles (ZnS NPs) using two capture agents, in order to improve the spectral properties of ZnS, for application purposes for future studies, such as ion detection of heavy metals from polluted waters. This study highlights the following:

- The formation of ZnS NPs, with two capture agents ($C_4H_{11}NO_3$ -TRIS-ST3 (25 mM alcoholic solution) and $C_{13}H_{14}N_2OS$ -DF (25 mM alcoholic solution) was performed by the chemical co-precipitation reaction, from the basic percussions, acetate zinc (25 mM) and sodium sulfide (25 mM) at $65^\circ C$ and magnetic stirring (2000 rpm) for 30 minutes. The precipitates obtained were separated by decantation, Et-OH (99.9%) was added to cleaning and then dried in the oven for 6 hours at $80^\circ C$. Samples of newly obtained material are marked with ZnS NPs-TRIS, ZnS NPs-DF and ZnS NPs, respectively.
- The XRD and FTIR spectra on the obtained samples confirm the formation of synthesized ZnS nanoparticles, presenting a cubic structure.
- The size of the crystals was calculated with the Scherrer equation and it was observed that the ZnS NPs formed are in the range of 4 and 9 nm, higher values for the ZnS NPs sample ($8.57 \pm 1 nm$) compared to the samples when the agents were used capture (NPs-TRIS = $4.28 \pm 1 nm$ and ZnS NPs-DF = $4.28 \pm 1 nm$), thus indicating an inhibition of the agglomeration of ZnS NPs obtained, by about 50%.
- SEM images obtained on ZnS NPs samples with and without capture of agents, show agglomerations of nanoparticles, with limitation in case of TRIS and DF use. The mean dimensions (d_{med}) were thus calculated and it was observed that for ZnS NPs the d_{med} is $32.5 \pm 2 nm$, and for ZnS NPs-TRIS are the d_{med} values of $39 \pm 2 nm$ and for ZnS NPs-DF d_{med} of $36.1 \pm 2 nm$.
- The EDX analysis confirmed on the surface of the nanoparticles the presence of Zn and S in all the obtained samples, but also specific elements of the capture agents.
- It was found that the optical structure and properties change after the use of the capture agent in the synthetic chemical reaction, by changes in UV-vis spectra, the calculated optical band (E_g) values, increasing from 3.71 eV for ZnS NPs, at 3.83 eV for ZnS NPs-TRIS and ZnS NPs-DF, respectively.
- The increase in conductivity over time, from $1047 \mu S/cm$ (ZnS NPs) to $1370 \mu S/cm$ (ZnS NPs-DF) and $1156 \mu S/cm$ (ZnS NPs-TRIS), indicates an improvement of the electrical properties of ZnS NPs, through the synthetic use of DF and TRIS capture agents.
- The materials studied in this paper, such as ZnS NPs, have different applications due to their confirmed activity.

- Improvements in optical properties, complemented by structural changes, obtained through the use of capture agents, can be useful as applications in areas such as: optoelectronics, photocatalysis, electrocatalysis, but also as sensors for detecting heavy metal ions.

Personal contributions

- The presented researches, original, which aimed to obtain new optimal results, which would contribute to the study of oxidative processes of some metal sulfides, in finding effective solutions to inhibit oxidative processes.
- Evaluation of the oxidation process of ZnS and identification of effective inhibitors for this material, acting with a yield of over 90% under optimal reaction conditions (pH 2.5 and 25°C), by identifying the organic compound DF3 that acts efficiently greater than 98%.
- Evaluation of the oxidation process of FeS and testing of two organic compounds as inhibitors of the oxidation reaction: glycine, which acts with an efficiency of more than 40% and, respectively, a new Schiff base grafted with TRIS units that act with an efficiency of 44% (compound ST1).
- Evaluation of the oxidation process of PbS and identification of inhibitors from the class of Schiff bases grafted with TRIS units, which act with inhibition efficiency higher than 60%, the most efficient being the structure of the compound ST3 (C₄H₁₁NO₃).
- Evaluation of the oxidation process of CuFeS₂ and presentation of effective inhibitors from the class of phenacyl derivatives with inhibition efficiency greater than 50%, and respectively from the class of Schiff bases grafted with TRIS units, indicating inhibition efficiency greater than 54%.
- Obtaining new materials of ZnS NPs type with two capture agents, organic compounds (DF1 and TRIS-ST3), which present structural changes and improved optical / spectral properties, which can offer applicability in various fields, such as: electrocatalysis, optoelectronics, photocatalysis and as sensory detectors for heavy metal ions.
- Personal development by deepening modern analysis techniques, by participating during the doctoral program, with scientific contributions to 11 national / international events, as well as to exchanges of ideas in an international project (international training in 2017, in the COST project- e-MINDS, <https://www.cost.eu/>).
- Capitalizing on the results obtained in 3 ISI scientific articles (cumulative impact factor of 11,178), of which 2 articles as first author (cumulative impact factor of 4,823) through successful collaboration with colleagues from the University of Craiova, University „Dunărea de Jos,, from Galați and the University „Al Cuza,, from Iași.

Perspectives in future research

- Investigation of the optimal concentration of inhibitors in oxidative processes in ZnS, organic inhibitors tested in the scientific approach (DF1, DF2 and DF3), but for concentrations higher than 1 mM, the results obtained indicating encouraging efficiencies for future studies.
- Initiation of applied research in zonal areas, affected by acid mining drainage in Romania, such as Zlatna area in Alba county and Copșa Mică area in Sibiu county,

- and in this sense, the studies will aim to obtain samples of metal sulfides in the area of interest and their testing in contact with inhibitors with newly synthesized structures.
- Testing applications of ZnS nanoparticles as sensors/selection probes for the detection of heavy metal ions in polluting waters affected by acid mining drainage in Zlatna and Copșa Mică areas, where high concentrations of heavy metals are recorded annually (Cu, Pb, Zn and Cd).
 - Obtaining new materials based on metal sulfide and directing their applicability to environmental protection.
 - Enrollment in future competitions with new research in a postdoctoral project and conducting an external research internship.

Dissemination of research results

Publications in ISI indexed journals

1. **Duinea I.M.**, Cârâc G., Dăbuleanu I., Petcu M., Laura S., Bîrsă L., Chiriță P.
Troilite (FeS) oxidation in the presence of a newly synthesized TRIS-based base.
Rev.Chim. (Bucharest) 70 (7) (2019) p. 2639-2642. (I.F. 1.605)
<https://revistadechimie.ro/pdf/68%20DUINEA%207%2019.pdf>
! <https://www.revistadechimie.ro/pdf/ERRATA.pdf>
2. Chiriță P., **Duinea I.M.**, Sandu A.M., Bîrsă L., Sârbu L., Baibarac M., Sava F., Popescu M., Matei E.
Inhibitory effect of three phenacyl derivatives on the oxidation of sphalerite (ZnS) in air-equilibrated acidic solution.
Corrosion Science, 138 (2018) p.154–162. (I.F. 6.355).
<https://www.sciencedirect.com/science/article/pii/S0010938X16314287>
3. **Duinea I.M.**, Sandu A.M., Petcu M., Dabuleanu I., Cârâc G., Chiriță P.
Aqueous oxidation of iron monosulfide (FeS) in the presence of glycine.
Journal of Electroanalytical Chemistry 804 (2017) p. 165–170. (I.F. 3.218)
<https://www.sciencedirect.com/science/article/pii/S1572665717307075>

Publications in journals indexed in international data bases

1. **Duinea M.I.**, Manea M., Sandu A.M., Ghejan B., Petcu M. și Chiriță P.
The oxidative dissolution of iron monosulfide (FeS): A Cyclic Voltammetry study.
Annals of the University of Craiova, The Chemistry Series, XLIV (2), 2017, p. 75-81. ISSN 1223-5288. <http://chimie.ucv.ro/departament/>
2. **Duinea M.I.**, Cârâc G., Dabuleanu I., Sandu A.M., Ghejan B., Bîrsă L.M., Chiriță P.
The inhibiting effect of Tris (hydroxymethyl) aminomethane (TRIS) on the corrosion of metal iron.
Annals of the University of Craiova 45, 2016, p 22-25. ISSN 1223-5288.
<http://chimie.ucv.ro/departament/>

Rewarding research results by UEFISCDI

1. Chiriță P., Duinea I.M., Sandu A.M., Bîrsă L., Sârbu L., Baibarac M., Sava F., Popescu M., Matei E.
Inhibitory effect of three phenacyl derivatives on the oxidation of sphalerite (ZnS) in air-equilibrated acidic solution.
Corrosion Science, 138 (2018) p.154–162. (I.F. 6.355).
<https://www.sciencedirect.com/science/article/pii/S0010938X16314287>,
Q1, I.F. 6.355, No., 142, List 8
<https://uefiscdi.gov.ro/resource-85015?&wtok=&wtkps=XY5dDolwEITvss+CbEsDLncgJp6A0Ib0BLKnxjvbsEHO0872cw3MwUI9HSkCOahaR1keeZIEjjW4FUcEaBauuSxKIHNYuphIQ1HU8xrgJUuyq4I0NaVvabHwl4u4JAIxiSu1imTA+bYaEQOvufR4cZRKJVKSRsnfCo9/PQSAqiShR7rFqp//Bv26X6Pvnc3e69XN6rE1oe3rcDQVU1JzOLGZw6lfuLR+8OsN&wchk=9560052de41a35da1b713412c36897d365a41f15>
2. Duinea I.M., Sandu A.M., Petcu M., Dabuleanu I., Cârâc G., Chiriță P.
Aqueous oxidation of iron monosulfide (FeS) in the presence of glycine.
Journal of Electroanalytical Chemistry 804 (2017) p. 165–170. (I.F. 3.218).
<https://www.sciencedirect.com/science/article/pii/S1572665717307075>
Q1, I.F. 3.218, No. 76, List 5
<https://uefiscdi.gov.ro/resource-87903%20?&wtok=9f1800a6a128a07d1738245a12568e31309f37e1&wtkps=XY7dDolwDEbfpdcG19WxUd7BmPqEuBWziGIYyIXx3eUnxuhVm+acr1/Flp+JDcPYX5oEZWRUBnFHeZmYGFIMMG+agYINeVFpFK+0NVpEeVcXJ6LKWRE7c8gQ5znhBmGN8GHNxWIGLEMI99vhuCWrtNNOGbcYk/q9bDSiURCWmLNYu3/HFQMv+D0d5RP4Wsbhkayitng9Qx+RCzR5Qxq7o++raB8vUG&wchk=fa148dfd9727836f132233ac0d9a32a493a0b94b>

Participation in national / international conferences

1. Duinea M.I., Chiriță P., Cârâc G. *Organic compounds with inhibitor effect in the oxidative process on metal sulphides surface.* A 8th Edition of Scientific Conference organized by the Doctoral Schools of “Dunărea de Jos” University of Galați (CSSD-UDJG 2020), Fifth Edition of Scientific Conference of Doctoral Schools from UDJ Galați, 13-14 Iunie 2020, Galați, România, oral presentation, S5/5.1/OP.6.7.
<http://www.cssd-udjq.ugal.ro/>
2. Duinea M.I., Cudulbeanu M., Chiriță P., Cârâc G. *Synthesis and characterization of ZnS nanoparticles for the detection of heavy metals ions.* A 8th Edition of Scientific Conference organized by the Doctoral Schools of “Dunărea de Jos” University of Galați (CSSD-UDJG 2020), Fifth Edition of Scientific Conference of Doctoral Schools from UDJ Galați, 13-14 Iunie 2020, Galați, România, oral presentation, S5/5.1/OP.6.8.
<http://www.cssd-udjq.ugal.ro/>
3. Duinea I.M., Cârâc G., Chiriță P., *Oxidative Dissolution of the metal sulfides (Me-S Type Materials) Using Organic Compounds* A 7th Edition of Scientific Conference organized by the Doctoral Schools of “Dunărea de Jos” University of Galați (CSSD-UDJG 2019), Fifth Edition of Scientific Conference of Doctoral Schools from UDJ Galați, 13-14 Iunie 2019, Galați, România, oral presentation, S5/5.1/OP.5.1.9.
<http://www.cssd-udjq.ugal.ro/>

4. **Duinea I. M.**, Cârâc G., Chirița P., *The Effect of Synthesized TRIS-based Schiff on the Oxidative Dissolution of Iron Monosulfide (FeS)* A 7th Edition of Scientific Conference organized by the Doctoral Schools of "Dunărea de Jos" University of Galați (**CSSD-UDJG 2019**), *Fifth Edition of Scientific Conference of Doctoral Schools from UDJ Galați*, 13 - 14 Iunie **2019**, Galați, România, poster presentation S5/5.1/PP.5.1.2.
<http://www.cssd-udjg.ugal.ro/>
5. **Duinea I. M.**, Cârâc G., Chirița P., Bîrsă L.M., *Efficient oxidation of metal sulfides using tris-based Schiff to construct advanced electrode active materials*. 20th Romanian International Conference on Chemistry and Chemical Engineering (**RICCCE 2019**) 4 – 7 September **2019** Mamaia-Constanța, România, poster presentation, S3/PP36.
<http://riccce20.chimie.upb.ro/>
6. **Duinea I. M.**, Cârâc G., Petcu A., Dăbuleanu I., Simionu A., Chirița P., *Dizolvarea oxidativa a sulfurilor metalice (MeS)*. A VIII-a ediție a Simpozionul Național de Chimie, Craiova, **2018**- oral presentation, S1/OP3.
<http://chimie.ucv.ro/simpchim/>
7. **Duinea I. M.**, Cârâc G., Ghigu Ș., Ghejan B., Sandu A.M., Dabuleanu I., Bîrsă L., Chirița P., *Inhibarea dizolvarii oxidative a monosulfurii de fier FeS*. XXXV-a Conferinta Nationala de Chimie, Călimanesti Căciulata, România, **2018** poster presentation, S3/PP5.
www.conferinta.oltchim.ro
8. **Duinea I. M.**, Cârâc G., Manea M., Chirița P., *The Oxidativ Dissolution of FeS in the presence of Glycine solution*. A 6th Edition of Scientific Conference organized by the Doctoral Schools of "Dunărea de Jos" University of Galați (**CSSD-UDJG 2018**), *Fifth Edition of Scientific Conference of Doctoral Schools from UDJ Galați*, 7 - 8 Iunie **2018**, Galați, România, poster presentation, S5/PP 5.1.4.
<http://www.cssd-udjg.ugal.ro/>
9. **Duinea I. M.**, Cârâc G., Ghejan B., Sandu A.M., Petcu M., Bîrsă L., Chirița P., *The Oxidativa Dissolution of Pyrite in the Presence of New Synthesized Organic Compounds*. International Conference on Chemical Engineering (ICCE), Iași, România, **2018**, poster presentation, S3/PP11.
www.ch.tuiasi.ro
10. **Duinea I. M.**, Cârâc G., Ghejan B., Sandu A.M., Bîrsă L., Chirița P., *The oxidativa dissolution of pyrite in the presence of 1-(5-bromo-2-hydroxyphenyl)-1-oxaethan-2-yl-N,N-diethyldithiocarbamate*. 20th Romanian International Conference on Chemistry and Chemical Engineering (RICCCE), Brașov, România, **2017**- poster presentation, S3/PP50.
<http://riccce20.chimie.upb.ro/>

11. **Duinea I.M.**, David D., Cârâc G. *Solvent effect in electrochemical properties of neodymium oxide of micro and nanoparticles*. A 5th Edition of Scientific Conference organized by the Doctoral Schools of "Dunărea de Jos" University of Galați (**CSSD-UDJG 2017**), Fifth Edition of Scientific Conference of Doctoral Schools from UDJ Galați, **2017**- oral presentation S3/OP 3.1.
<http://www.cssd-udjg.ugal.ro/>
12. **Duinea I. M.**, Sandu A.M., Petcu M., Ghejan B., Simionu A., Cârâc G., Chiriță P., *Dizolvarea oxidativă a unor materiale de tipul sulfurilor minerale*. A 9-a ediție a Simpozionul Național de Chimie, Craiova, România, 27 Noiembrie **2017**- oral presentation S1/OP2.
<http://chimie.ucv.ro/simpchim/>
13. **Duinea I.M.**, Cârâc G., Ghejan B., Sandu A.M., Petcu A., Chiriță P., *Dizolvarea oxidativă a FeS₂ în prezența histidinei*. A 8-a ediție a Simpozionul Național de Chimie, Craiova, 26 Noiembrie **2016** România, oral presentation S1/ OP6.
<http://chimie.ucv.ro/simpchim/>

Activity in scientific research

1. **Research technician** in the research project PN-II-PT-PCCA 51/2012 (**2016**) "*The study of the effect of organic complexing agents of Fe (III) or Fe (II) on iron oxidative monosulfides*" from the University of Craiova, project director Conf. Dr. Paul Chiriță.
<http://www.chem.uaic.ro/files/File/ecafe/Project.html>
2. **Research assistant** - doctoral student in the research project PN III no. 75PED / **2017** „*Advanced anodic materials for improved performance and durability*„ from the University of Craiova, project director Lect. Dr. Nicoleta Cioateră.
<http://chimie.ucv.ro/expand/index.htm>
3. **Participation in international training** - Electrochemical processing methodologies and corrosion protection for device and systems miniaturization (**e-MINDS**). Training School, Schwäbisch Gmünd, Germany, April 2-6, **2017**.
<https://www.e-minds.ch/>

Selective Bibliography

- [1] **M.I. Duinea**, A.M. Sandu, M.A. Petcu, I. Dăbuleanu, G. Cârâc, P. Chiriță, *Aqueous oxidation of iron monosulfide (FeS) in the presence of glycine*, J. Electroanal. Chem. 804 (2017) 165–170.
- [2] M. Keim, G. Markl. *Weathering of galena: mineralogical processes, hydrogeochemical fluid path modeling, and estimation of the growth rate of pyromorphite*. Am Miner 100 (2015) 1584–1594.
- [3] L. George, N. Cook, C. Ciobanu, B. Wade. *Trace and minor elements in galena: a reconnaissance LA-ICP-MS study*. Am Miner 100(2–3) (2015) 548–569.
- [4] P. Chiriță, **M.I. Duinea**, A. Sandu, L. Bîrsă, L. Sarbu, M. Baibarc, F. Sava, M. Popu, E. Matei, Inhibitory effect of three phenacyl derivatives on the oxidation of sphalerite (ZnS) in air-equilibrated acidic solution, Corrosion Science, 138 (2018) 154–162.

- [5] **M.I. Duinea**, G. Cârâc, I.D. Dăbuleanu, M.A. Petcu, L.G. Sarbu, M.L. Bîrsă, P. Chiriță. *troilite (FeS) oxidation in the presence of a newly synthesized TRIS-based base*. Rev.Chim. (Bucharest). 70 (7) (2019) 2639-2642.
- [6] C.G. Weisener, R.St.C. Smart, A.R. Gerson, *Kinetics and mechanisms of the leaching of low Fe sphalerite*, Geochim. Cosmochim. Acta 67 (2003) 823–830.
- [7] C.G. Weisener, R.St.C. Smart, A.R. Gerson, *A comparison of the kinetics and mechanism of acid leaching of sphalerite containing low and high concentrations of iron*, Int. J. Miner. Process. 74 (2004) 239–249.
- [8] S. Ghassa, H. Abdollahi, M. Gharabaghi, S. C. Chelgani, M. Jafari, *The Surface Chemistry Characterization of Pyrite, Sphalerite and Molybdenite after Bioleaching*, 22nd International Biohydrometallurgy Symposium, 262 (2017) 487-491, ISSN: 1662-9779.
- [9] Y. Li, G. Qian, J. Li, A.R. Gerson, *Kinetics and roles of solution and surface species of chalcopyrite dissolution at 650 mV*, Geochim. Cosmochim. Acta 161 (2015) 188–202.
- [10] Y. Mikhlin, Y. Tomashevich, *Pristine and reacted surfaces of pyrrhotite and arsenopyrite as studied by X-ray absorption near-edge structure spectroscopy*, Phys. Chem. Miner. 32 (2005) 19–27.
- [11] A.R. Pratt, I.J. Muir, H.W. Nesbitt, *X-ray photoelectron and Auger electron spectroscopic studies of pyrrhotite and mechanism of air oxidation*, Geochim. Cosmochim. Acta 58 (1994) 827–841.
- [12] T. Tuken, B Yazıcı, M. Erbil, *The corrosion behaviour of polypyrrole coating synthesized in phenylphosphonic acid solution*. Appl. Surf. Sci., 252 (2006) 2311-2318.
- [13] P. Chiriță, *Iron monosulfide (FeS) oxidation by dissolved oxygen: Characteristics of the product layer*. Surf. Interface Anal. 41 (2009) 405–411.
- [14] P. Chiriță, M. Dostes, M.L. Schlegel, *Oxidation of FeS by oxygen-bearing acidic solutions*. J. Colloid Interface Sci. 321 (2008) 84–95.
- [15] L.C. Roberts, S.J. Hug, T. Ruettimann, M.M. Billash, A.W. Khan, M.T. Rahman, *Arsenic removal with iron(II) and iron(III) in waters with high silicate and phosphate concentrations*. Environ. Sci. Technol., 38 (2004) 307–315.
- [16] C.A. Constantin, P. Chiriță, C.E. Badica, L.M. Bîrsă, E. Matei, I. Baltog, M.L. Schlegel, *The effect of some new organic inhibitors on the oxidative dissolution of iron monosulfide (FeS)*. Goldschmidt Conference 2013, Florence, Italy, August 25-30, 2013.
- [17] C.M.V.B. Almeida, B.F. Giannetti, *A new and practical carbon paste electrode for insoluble and ground samples*, Electrochem. Commun. 4 (2002) 985–988.
- [18] P. Chiriță, *Aqueous oxidation of iron monosulfide (FeS) by molecular oxygen*, Miner. Process. Extr. Metall. Rev. 37 (2016) 305–310.
- [19] **M.I. Duinea**, C.E. Badica, M.L. Schlegel, P. Chiriță, *Effect of sulfosalicylic acid on iron monosulfide (FeS) oxidativa dissolution in aerated acidic solutions*. Goldschmidt 8-13 iunie 2014, Sacramento, SUA, (www.goldschmidt.com)
- [20] C.E. Badica, **M.I. Duinea**, L.M. Bîrsă, M.A. Baibarac, E. Matei, P. Chiriță, *The effect of some synthetic organic compounds on the oxidativa dissolution of iron monosulfide (FeS)*. Book of abstracts. 24th Annual V.M. Goldschmidt Conference Sacramento, (2014) 95.
- [21] **M.I. Duinea**, G. Cârâc, I. Dabuleanu, A.M. Sandu, B. Ghejan, L.M. Bîrsă, P. Chiriță, *The inhibiting effect of Tris (hydroxymethyl) aminomethane (TRIS) on the corrosion of metal iron*, Annals of the University of Craiova. XLIII, 1 (2016) 48-53.
- [22] R. Rossetti, R. Hull, J.M. Gibson, L.E. Brus, *Excited electronic states and optical spectra of ZnS and CdS crystallites in the 15 to 50 Å size range: Evolution from molecular to bulk semiconducting properties*. J. Chem. Phys. (1985) 82, 552–559.
- [23] M. Kuppayee, G. Vanathi, K. Nachiyar, V. Ramasamy, *Synthesis and characterization of Cu²⁺ doped ZnS nanoparticles using TOPO and SHMP as capping agents*, Appl. Surf. Sci. 257 (2011) 6779.

- [24] H.F. Steger, L.E. Desjardins, *Oxidation of sulfide minerals, 4. Pyrite, chalcopyrite and pyrrhotite*, Chem. Geol. 23 (1978) 225–237.
- [25] M. El Belghiti, Y. Karzazi, A. Dafali, B. Hammouti, F. Bentiss, I.B. Obot, I. Bahadur, E.E. Ebenso, *Experimental, quantum chemical and Monte Carlo simulation studies of 3,5-disubstituted-4-amino-1,2,4-triazoles as corrosion inhibitors on mild steel in acidic medium*, J. Mol. Liq. 218 (2016) 281–293.
- [26] S.N. White, *Laser Raman spectroscopy as a technique for identification of seafloor hydrothermal and cold seep minerals*, Chem. Geol. 259 (2009) 240–252.
- [27] Y. C. Cheng, C.Q. Jin, F. Gao, X.L. Wu, W. Zhong, S.H. Li, P.K. Chu, *Raman scattering study of zinc blende and wurtzite ZnS*, J. Appl. Phys., 106 (2009) 123505.
- [28] P. Chiriță, A. Samide, O. Rusu, M. Preda, *Investigations on the oxidativa degradation of pyrite with hydrogen peroxide in phosphate medium*, Rev. Chim. 54 (2003) 950–953.
- [29] J.E. Thomas, R.St.C. Smart, W.M. Skinner, *Kinetic factors for oxidative and non-oxidative dissolution of iron sulfides*. Minerals Engineering 13 (2000) 1149-1159.
- [30] P. Acero, J. Cama, C. Ayora, *Sphalerite dissolution kinetics in acidic environment*, Appl. Geochem. 22 (2007) 1872–1883.
- [31] G.J. Janz, J.W. Coutts, J.R. Downey, E. Roduner, *Raman studies of sulfur-containing anions in inorganic polysulfides*. Potassium polysulfides, Inorg. Chem. 15 (1976) 1755–1759.
- [31] P. Chiriță, C.E. Badica, C.A.† Constantin, L.M. Bîrsă, E. Matei, M. Baibarac, *Influence of 2,2'-bipyridine on oxidative dissolution of iron monosulfide*. Surf. Interface Anal. 46 (2014) 842–846.
- [32] **M.I. Duinea**, M. Manea, A. Sandu, B. Ghejan, M. Petcu, P. Chiriță, *The oxidativa dissolution of iron monosulfide (FeS): A Cyclic Voltammetry study*, Annals of the University of Craiova, The Chemistry Series, XLIV (2) (2017) 75-81.
- [33] W. Qafsaoui, M.W. Kendig, H. Perrot, H. Takenouti, *Coupling of electrochemical techniques to study copper corrosion inhibition in 0.5 mol L⁻¹ NaCl by 1-pyrrolidine dithiocarbamate*, Electrochim. Acta 87 (2013) 348–360.
- [34] **M.I. Duinea**, A.M. Sandu, M.A. Petcu, I. Dăbuleanu, G. Cârâc, P. Chiriță, *Aqueous oxidation of iron monosulfide (FeS) in the presence of glycine*, J. Electroanal. Chem. 804 (2017) 165–170.
- [35] C.B. Tabelin, S. Veerawattananun, M. Ito, N. Hiroyoshi, T. Igarashi, *Pyrite oxidation in the presence of hematite and alumina: II. Effects on the cathodic and anodic half-cell reactions*, Sci. Total Environ. 581–582 (2017) 126–135.
- [36] A. Ata, K. Soner, *Acid Mine Drainage (AMD): causes, treatment and case studies*. J. Clean. Prod. 14 (2006) 1139-1145.
- [37] J. Liu, D. A. Aruguete, J. R. Jinschek, J. D. Rimstidt, M. F. Hochella, *The non-oxidative dissolution of galena nanocrystals: Insights into mineral dissolution rates as a function of grain size, shape, and aggregation state*. Geochim. Cosmochim. Acta 72 (2008) 5984–5996.
- [38] D.T. Juravle, *Geologie Generală*. Editura STEF Iași. (2015) 157-178, ISBN: 978-606-575-513-0.
- [39] C. Heidel, M. Tichomirowa, C. Breitung, *Sphalerite oxidation pathways detected by oxygen and sulfur isotope studies*, Appl. Geochem. 26 (2011) 2247–2259.
- [40] F. Frau, C. Ardaù, L. Fanfani, *Environmental geochemistry and mineralogy of lead at the old mine area of Baccu Locci (south-east Sardinia, Italy)*. J. Geochem. Explor. (2009) 100, 105–115.
- [41] A.A. Chen, *Kinetics of leaching galena concentrates with ferric fluorsilicate solution*, (1992) 10-70.
- [42] M.B.J. Lindsay, P.D. Condon, J.L. Jambor, K.G. Lear, D.W. Blowes, C.J. Ptacek, *Mineralogical, geochemical, and microbial investigation of a sulfide-rich tailings deposit characterized by neutral drainage*. Appl. Geochem. 24 (2009) 2212–2221.
- [43] R. Woods, *Oxidation of ethyl xanthate on platinum, gold, copper, and galena electrodes. Relation to the mechanism of mineral flotation*, J. Phys. Chem. 75 (1971) 354–362.

- [44] A. Ruiz-Sanchez, G.T. Lapidus, *Study of chalcopyrite leaching from a copper concentrate with hydrogen peroxide in aqueous ethylene glycol media*. Hydrometallurgy, 169 (2017) 192-200.
- [45] J. Hu, G. Tian, F. Zi, X. Hu, *Leaching of chalcopyrite with hydrogen peroxide in 1-hexyl-3-methylimidazolium hydrogen sulfate ionic liquid aqueous solution*. Hydrometallurgy, 169 (2017) 1-8.
- [46] C.A. Constantin, P. Chiriță, *Oxidativa dissolution of pyrite in acidic media*, J. Appl. Electrochem. 43 (2013) 659–666.
- [47] X. Peng, L. Manna, W. Yang, J. Wickham, E. Scher, A. Kadavanich, A. Alivisatos, *Shape control of CdSe nanocrystals*, Nature 404 (2000), 59–61.
- [48] X. Fang, T. Zhai, U.K. Gautam, *ZnS nanostructures: from synthesis to applications*, Progress in Materials Science, 56, 2 (2011) 175–287.
- [49] R. Zein, I. Alghoraibi, *Influence of Bath Temperature and Deposition Time on Topographical and Optical Properties of Nanoparticles ZnS Thin Films Synthesized by a Chemical Bath Deposition Method*, Journal of Nanomaterials (2019) 13.
- [50] D. Ayodhya, G. Veerabhadram, *Fabrication of Schiff base coordinated ZnS nanoparticles for SHEanced photocatalytic degradation of chlorpyrifos pesticide and detection of heavy metal ions*. Journal of Materiomics. 5, 3 (2019) 446-454.
- [51] M.B. Zaman, T. Chandel, K. Dehury, P. Rajaram, *Synthesis and characterization of spin-coated ZnS thin films*, AIP Conference Proceedings 1953 (2018) 100066.
- [52] F. Zhong, Z. Wu, J. Guo, D. Jia, *Ni-doped ZnS nanospheres decorated with Au nanoparticles for highly improved gas sensor performance*, Sensors, 18, 9 (2018) 2882.
- [53] N. Kaur, S. Kaur, J. Singh, M. Rawat, *A review on zinc sulphide nanoparticles: from synthesis, properties to applications*,” Journal of Bioelectronics and Nanotechnology, 1, 1 (2016) 5.
- [54] S. Pratap, J. Prasad, R. Kumar, K. Murari, S. S. Singh, *Preparation and characteristics of IR window grade zinc sulphide powder*,” Defence Science Journal, 46,4 (1996) 215– 22.
- [55] X. Yan G. Feng, C. Yang, S. Wang, S. Zhou, *Random lasing in Cr:ZnS microstructure-textured grooves*, Laser Physics, 26, 4 (2016) 045702.
- [56] H.C. Chien, C.-Y. Cheng, M.-H. Mao, *“Continuous wave operation of SiO₂ sandwiched colloidal CdSe/ZnS quantumdot microdisk lasers*, IEEE Journal of Selected Topics in Quantum Electronics, 23, 5 (2017) 1–5.